INFN-AE-05-08
SLAC-PUB-11676
physics/0512235

**20 Dicembre 2005**

**INFN Roadmap Report**

# *SuperB*: a linear high-luminosity *B* Factory

J. Albert,[1] S. Bettarini,[2] M. Biagini,[3] G. Bonneaud,[4] Y. Cai,[5] G. Calderini,[2] M. Ciuchini,[6] G. P.Dubois-Felsmann,[1] S. Ecklund,[5] F. Forti,[2] T. J. Gershon,[7] M. A. Giorgi,[2] D. G. Hitlin,[1] D. W. G. S. Leith,[5] A. Lusiani,[2] D. B. MacFarlane,[5] F. Martinez-Vidal,[8] N. Neri,[2] A. Novokhatski,[5] M. Pierini,[9] G. Piredda,[10] S. Playfer,[11] F. C. Porter,[1] P. Raimondi,[3] B. N.Ratcliff,[5] A. Roodman,[5] J. Seeman,[5] L. Silvestrini,[10] A. Stocchi,[12] M. Sullivan,[5] U. Wienands,[5] and W. J. Wisniewski[5]

[1]*California Institute of Technology, Pasadena, CA 91125, USA*
[2]*Università di Pisa, Dipartimento di Fisica, Scuola Normale Superiore and INFN, I-56127 Pisa, Italy*
[3]*Laboratori Nazionali di Frascati dell'INFN, I-00044 Frascati, Italy*
[4]*Ecole Polytechnique, LLR, F-91128 Palaiseau, France*
[5]*Stanford Linear Accelerator Center, Stanford, CA 94309, USA*
[6]*Università di Roma Tre, Dipartimento di Fisica and INFN, I-00146 Roma, Italy*
[7]*Department of Physics, University of Warwick, Coventry CV4 7AL, United Kingdom*
[8]*IFIC, Universitat de Valencia-CSIC, E-46071 Valencia, Spain*
[9]*University of Wisconsin, Madison, Wisconsin 53706, USA*
[10]*Università di Roma La Sapienza, Dipartimento di Fisica and INFN, I-00185 Roma, Italy*
[11]*University of Edinburgh, Edinburgh EH9 3JZ, United Kingdom*
[12]*Laboratoire de l'Accélérateur Linéaire, F-91898 Orsay, France*

## Abstract

This paper is based on the outcome of the activity that has taken place during the recent workshop on "*SuperB* in Italy" held in Frascati on November 11-12, 2005. The workshop was opened by a theoretical introduction of Marco Ciuchini and was structured in two working groups. One focused on the machine and the other on the detector and experimental issues.*

The present status on *CP* is mainly based on the results achieved by *BABAR* and *Belle*. Estabilishment of the indirect *CP* violation in *B* sector in 2001 and of the direct CP violation in 2004 thanks to the success of PEP-II and KEKB $e^+e^-$ asymmetric *B* Factories operating at the center of mass energy corresponding to the mass of the $\Upsilon(4S)$. With the two *B* Factories taking data, the Unitarity Triangle is now beginning to be overconstrained by improving the measurements of the sides and now also of the angles $\alpha$, and $\gamma$. We are also in presence of the very intriguing results about the measurements of $\sin 2\beta$ in the time dependent analysis of decay channels via penguin loops, where $b \to s\bar{s}s$ and $b \to s\bar{d}d$. $\tau$ physics, in particular LFV search, as well as charm and ISR physics are important parts of the scientific program of a *SuperB* Factory. The physics case together with possible scenarios for the high luminosity *SuperB* Factory based on the concepts of the Linear Collider and the related experimental issues are discussed.

*PARTICIPANTS: Justin Albert, David Alesini, Virginia Azzolini, Rinaldo Baldini Ferroli, Marica Biagini, Caterina Biscari, Yunhai Cai, Giovanni Calderini, Massimo Carpinelli, Marco Ciuchini, Alessia D'Orazio, Riccardo De Sangro, Emanuele Di Marco, Riccardo Faccini, Giuseppe Finocchiaro, Francesco Forti, Yoshihiro Funakoshi, Alessandro Gallo, Tim Gershon, Marcello Giorgi, Susanna Guiducci, David Hitlin, Toru Iijima, David Leith, Eugene Levichev, Luigi Li Gioi, David MacFarlane, Fernando Martinez Vidal, Nicola Neri, Sergey Nikitin, Fernando Palombo, Ida Peruzzi, Marcello Piccolo, Maurizio Pierini, Pavel Piminov, Giancarlo Piredda, Steve Playfer, Andrea Preger Miro, Pantaleo Raimondi, Aaron Roodman, Emmanuele Salvati, John Seeman, Dmitry Shatilov, Michael Sullivan, John Walsh, Andy Wolsky, Mikhail Zobov

PACS: 12.15.Hh, 13.25.Hw, 13.35.Dx, 29.17.+w



Work supported in part by Department of Energy contract DE-AC02-76SF00515

### OUTLINE OF THE DOCUMENT

This document is divided in three sections:

- part one: physics motivations
- part two: experimental issues from "Detector Working Group"
- part three: machine issues from "Accelerator Working Group"

# Part I
# Overview and Physics Introduction

### 1. PRESENT *BABAR* AND *BELLE* PERFORMANCE

The two existing asymmetric $B$ Factories, PEP-II and KEKB, started their operations in 1999 and since then their design peak luminosities have been exceeded: now PEP-II is running with a peak luminosity of $10.5 \times 10^{33}\ cm^{-2}\ s^{-1}$ and KEKB with $15.8 \times 10^{33}\ cm^{-2}\ s^{-1}$. These terrific luminosities have been obtained also thanks to the continuous beam injection that both laboratories have assumed as normal operation mode.

Both machines achieved a tremendous increase in the integrated luminosity soon after the beginning of the operations in 1999 when both machines started to work in factory mode. Their peak luminosities exceed soon $10^{33}\ cm^{-2}\ s^{-1}$ , and the integrated luminosities of both $B$ Factories doubled every 2 years as shown in figure (1). At present the total integrated luminosity recorded by the two experiments (330 $fb^{-1}$ of *BABAR* and the 500 $fb^{-1}$ of *Belle*) is not too far from one billion of $B\bar{B}$ pairs.

### 2. DETECTORS CHARACTERISTICS

Both *BABAR* and *Belle* detectors are conceptually similar, they appear at first glance as the typical hermetic apparata designed for $e^+e^-$ colliders, made of an inner Vertex Detector, a Tracking system, an Electromagnetic Calorimeter, a Solenoidal Magnet and a Muon/Hadron system. Actually they show a clear asymmetry that is a consequence of the machine energy asymmetry. The distribution of the decay products in the laboratory system is in fact peaked in the forward direction, the direction of the high energy beam.

The more relevant differences of *Belle* with respect to *BABAR* are in the Silicon Vertex Tracker (a lower number of layers), in the Cherenkov system (Aerogel instead of the imaging internal reflection quartz DIRC) and glass instead of bakelite RPC for muon detection.

### 3. CKM CONSTRAINTS FROM NEW MEASUREMENTS OF THE SIDES AND ANGLES

The measurement of sin$2\beta$ became a program of precision measurements in the general fits of the CKM matrix in the $(\bar{\rho}, \bar{\eta})$ plane already in 2004 [1]. More challenging were the extractions of the other two angles of the unitarity triangle $\gamma$ and $\alpha$. New values of $|V_{ub}|$ and $|V_{cb}|$ [2], a new value of sin$2\beta$ from charmonium [3], the measurements of $\alpha$ [4] and $\gamma$ [5] have been presented last summer at LP05 and EPS05. They are in fact becoming the most stringent constraints of the Unitarity Triangle in the $(\bar{\rho}, \bar{\eta})$ plane [6], as shown in the figure (3). For this plot the information on $\cos 2\beta$, $\Delta m_d$, $\Delta m_s$ and the direct CP violation in the kaon sector $\epsilon_K$ are also used. We also show the impact of the measurements of the angles from the $B$ factories in the right plot of figure (3). The agreement between this bounds and the global area coming from sides measurements is an important test of the consistency of the CKM mechanism in describing non-leptonic $B$ decays and CP asymmetries. Present data suggest a (not yet significative) discrepancy, which calls for more data to be clarified in details.

Making the hypothesis that NP enters observables in the flavour sector only at the loop level, it is possible to determine the $\bar{\rho} - \bar{\eta}$ plane independently of NP contributions (see Figure 4), using tree-level $B$ decays : $V_{ub}$ and $V_{cb}$ using semileptonic inclusive and exclusive $B$ decays and the angle $\gamma$ measuring the phase of $V_{ub}$ appearing in the interference between $b \to c$ and $b \to u$ transitions to $DK$ final states.

The abundance of information allows to generalize the UT fit beyond the Standard Model, parameterizing in a general way the effect of New Physics (NP) through a multiplicative factor to the amplitude ($C_{B_d}$) and an additional weak phase ($\phi_{B_d}$) in the $B$–$\bar{B}$ mixing process [7]. As the left plot of figure (4) shows, even in this case the present measurements give a good constrain on $\bar{\rho}$ and $\bar{\eta}$, strongly suppressing the possibility of large NP enhancements in this sector (the fit gives a fraction of 7% probability for the NP solution with negative $\bar{\eta}$, respect to the 93% of the "Standard Model like" solution) [8]. This means that a huge increase in luminosity is needed, in order to discrimate NP scenarios from a simple Standard Model fit. This is more evident on the right plot of figure (4), where the present bound on the $\phi_{B_d}$ *vs.* $C_{B_d}$ plane is shown. In this case, in fact, the level of precision is not good enough to obtain any exclusion of the Standard Model scenario ($C_{B_d} = 1$ and $\phi_{B_d} = 0$).

In Summer 2004, the first observation of the asymmetry

$$A_{CP} = \frac{N(\bar{B}^0 \to K^-\pi^+) - N(B^0 \to K^+\pi^-)}{N(\bar{B}^0 \to K^-\pi^+) + N(B^0 \to K^+\pi^-)}$$

gave the evidence of direct CP violation in the $B$ sector. *BABAR* found an asymmetry value of

$$A_{CP} = -0.133 \pm 0.030_{Stat} \pm 0.009_{Syst}.$$

The value, after the average of *BABAR*, *Belle*, and CDF results, is [9]

$$A_{CP} = -0.114 \pm 0.020.$$

TABLE I: PEP-II and KEKB design parameters.

| Parameter | PEP-II | KEKB |
|---|---|---|
| Peak Lumi | $3.0 \times 10^{33}$ cm$^{-2}$s$^{-1}$ | $1.0 \times 10^{34}$ cm$^{-2}$s$^{-1}$ |
| $e^+$ Energy | 9.0 GeV | 8.0 GeV |
| $e^-$ Energy | 3.1 GeV | 3.5 GeV |

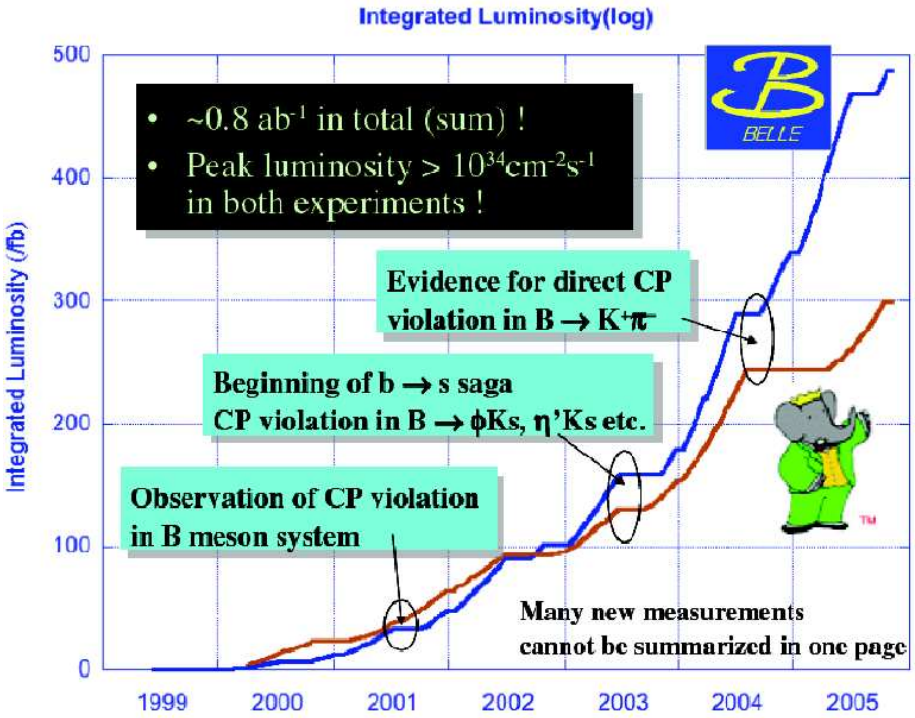


FIG. 1: Integrated luminosities delivered by PEP-II and by KEKB.

Starting in 2005 we have moved from the *CP* Violation discovery era (given by the asymmetries from time dependent and time integrated analyses as in the case of the direct CP violation in $B^0 \to K^+\pi^-$ , or in $B^+$ analysis for the extraction of $\gamma$), to a new era of precision measurements and constraints on the Unitarity Triangle.

## 4. MEASUREMENTS OF sin2$\beta$ VIA PENGUIN-MEDIATED DECAYS

An interesting field under study is the time-dependent analysis of those decay channels that can only proceed through "*penguin*" diagrams, such as the $b \to (s\bar{s}s)$ processes:

- $B^0 \to \phi K^0$
- $B^0 \to (KK)_{CP} K^0$

and the similar ($b \to (d\bar{d}s)$) transitions:

- $B^0 \to \eta' K^0$
- $B^0 \to f_0 K^0$
- $B^0 \to \pi^0 K^0$
- $B^0 \to \rho^0 K^0$
- $B^0 \to \omega K^0$.
- $B^0 \to \pi^0\pi^0 K^0$

These decays take the dominant contribution from the combination of CKM elements $V_{tb}V_{ts}^*$ and have the same phase of the charmonium channels $b \to (c\bar{c}s)$, up to a small phase shift of $V_{ts}$ respect to $V_{cb}$. If, however, new heavy quanta contribute to the loops (as shown in figure (5) in the case of SUSY), new phases can contribute to the asymmetry and the $S$ coefficient of the time dependent analysis could be substantially different from sin2$\beta$ [10]. The comparison between results from all the above $B^0$ decay channels [11] and sin2$\beta$ from charmonium, as shown in the HFAG plot (see

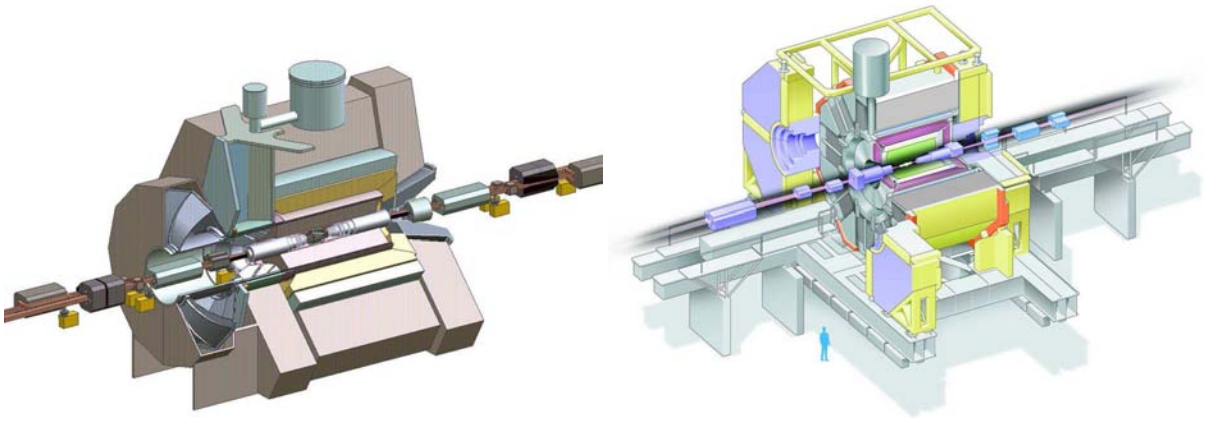

FIG. 2: *BABAR* and *Belle* detectors

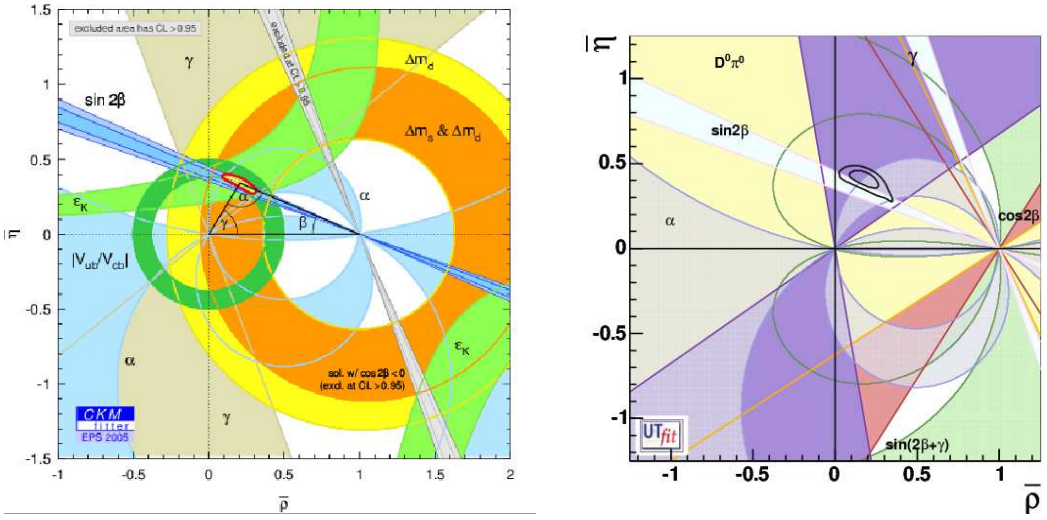


FIG. 3: $\bar{\rho}$, $\bar{\eta}$ plane using all the available constraints (left) and only the information from the UT angles (right).

Figure 6), must be interpreted anyway "*cum grano salis*". There are in fact other contributions to be taken into account in addition to the diagrams with top quark insertion in the loop.

For example, even in the case the theoretically cleanest channels ($B^0 \to \phi K^0$ and $B^0 \to K_S^0 K_S^0 K_S^0$), one has to take into account a Standard Model uncertainty due to a penguin contribution with an *up* quark running in the loop. Using the CKM couplings to scale this term to the leading contribution, we obtain a correction of the order of $\lambda^2 \approx 5\%$ coming from the fact that these contributions are doubly Cabibbo suppressed. For the other decay channels the uncertainty could be as large as 10% (or even more), since in that case the doubly Cabibbo suppressed terms also include tree-level transitions. [12]

Once these contributions are taken into account, one can use the experimental results for the $S$ parameters to obtain a bound on NP parameters [13]. For example, one can use the knowledge of $b \to s\gamma$ and $b \to sll$ Branching Ratios in SUSY models to bound the values of NP parameters and study their effect on the $b \to s$ penguin modes [14]. This is done in figure (7), where the case of a *RL* mass insertion

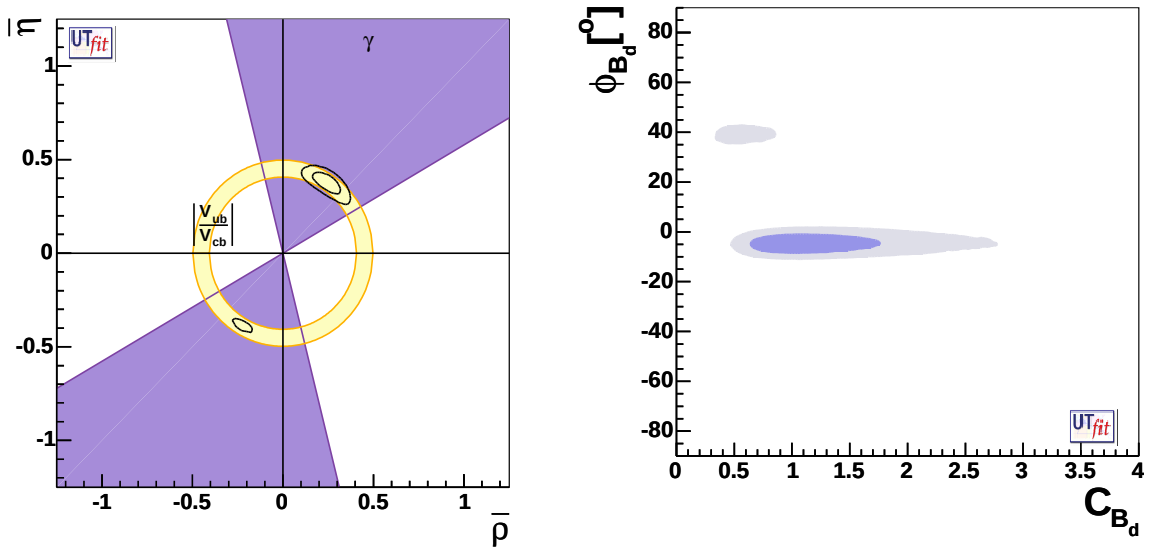


FIG. 4: Left:$\bar{\rho}$, $\bar{\eta}$ plane in a NP generalized scenario. Right: corresponding bound on NP parameters $\phi_{B_d}$ and $C_{B_d}$ (see text)

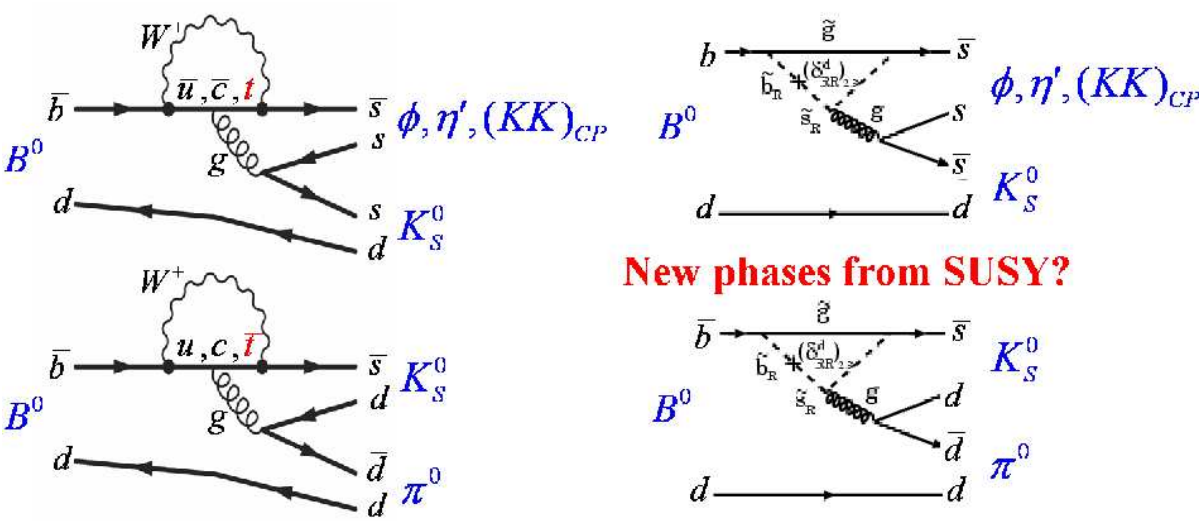


FIG. 5: Penguin diagrams.

in the squark propagator (inducing a transition from $\tilde{b} \to \tilde{s}$ transition) is taken into account.[1] The left plot of the figure shows the present knowledge on the $Im(\delta^{23}_{RL})$vs.$Re(\delta^{23}_{RL})$ from $BR(b \to s\gamma)$ and $BR(b \to sll)$, while the right plot gives $S(\phi K^0)$ as a function of $Im(\delta^{23}_{RL})$.

Many channels have been explored so far, some of them with poor statistics, some other richer. It is clear that we are at the beginning of a very interesting season when we can start probing the Standard Model in the flavour sector. In order to make this comparison really possible, the statistical error should be reduced below the theoretical uncertainties. To do that, a statistics between 20 and 50 times higher than present (i.e. 15 to 40 ab$^{-1}$) is needed. In few years, with LHC running and just before the beginning of the ILC project, a program of precision measurement at a *SuperB* with a capability of delivering more than a few tens of billions of $B\bar{B}$

[1] In SUSY models, the quark field rotation that generates the CKM matrix in the Standard Model, diagonalizing the quark mass matrix, also acts on squark mass matrix. Differently than for quark, squark mass matrix is not necessarily diagonalized by this rotation. Mass insertions are complex parameters representing the residual off-diagonal terms of the matrix. [15]

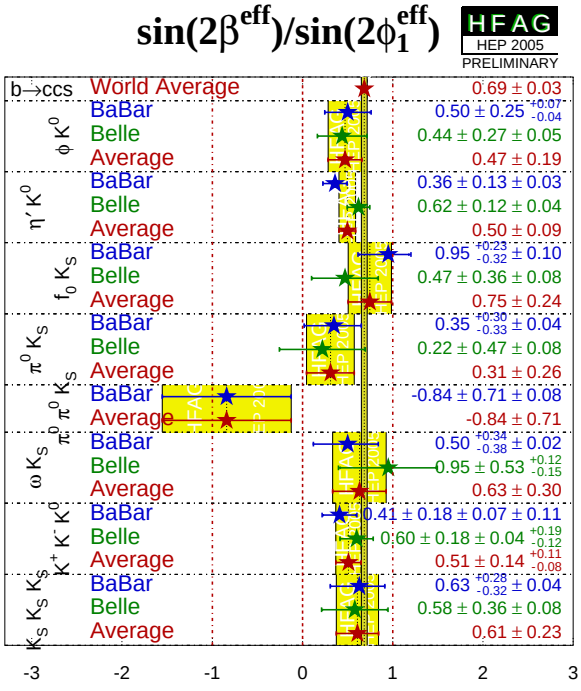


FIG. 6: Data for sin2$\beta$ effective, comparing $b \to c\bar{c}s$ and $b \to s\bar{s}s$ ($b \to d\bar{d}s$).

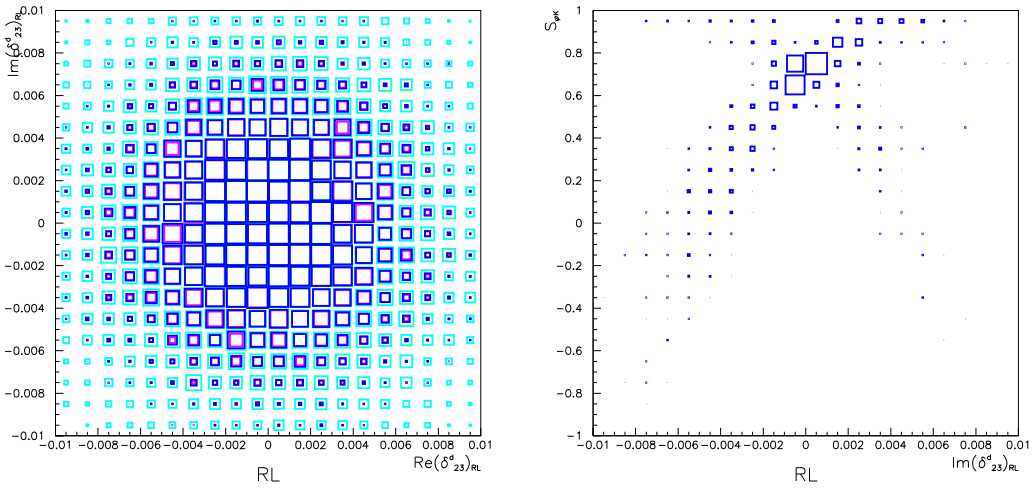


FIG. 7: Left: present bound on $Im(\delta^{23}_{RL})$vs.$Re(\delta^{23}_{RL})$ from $BR(b \to s\gamma)$ and $BR(b \to sll)$. Right: $S(\phi K^0)$ as a function of $Im(\delta^{23}_{RL})$ using the previous bound.

pairs, will be complementary to LHC physics. For example, the precise measurement of channels mediated by loop diagrams, both in $b \to s$ and $b \to d$ transitions, will allow to determine the couplings for New Physics contributions, such as the mass insertion parameters $\delta^{23}$ and $\delta^{13}$ in SUSY scenarios. For instance, a mass insertion $\delta^{23}$ with an imaginary part of $\sim 2\%$, with an average squark mass in the range $\sim 350 - 450$ GeV can produce a deviation of $S(\phi K^0_s)$ of the order of 20% respect to $S(J/\psi K^0_s - \phi K^0_s)$, as shown in the right plot of figure (7). In order to establish such 20% difference at the $5\sigma$ level, *i.e.* measuring $A_{CP}(\phi K^0_s) = 0.60 \pm 0.03$, and assuming the current per event sensitivity, we need to integrate a statistics corresponding to 30 ab$^{-1}$.

Similar constraints on New Physics can be obtained studying similar channels. For instance, the radiative penguin decays $b \to s\gamma$ provide a particularly clean environment. Direct *CP* violation in these decays is expected to be $\approx 0.5\%$ in the Standard Model, but could be enhanced by New Physics contributions to the penguin loop. Recent inclusive and exclusive measurements are just beginning to constrain such contributions. The information they provide at this point exclude the possibility of huge variations respect to the Standard Model expectations. On the other side, because of the limited statistics, the possibility of observing an enhancement of an order of magnitude is still open, but only a *SuperB* factory can provide the needed statistics. It is also important to stress the fact that CP measurements are statistics limited, and will continue to be so until at least 10 $ab^{-1}$. With larger samples it would be interesting to measure the direct *CP* asymmetry in $b \to d\gamma$ decays where the Standard Model prediction is -12%. *BABAR* has also shown that it is feasible to measure time-dependent *CP* violation in $B^0 \to K^{*0}(\to K^0_S\pi^0)\gamma$. In the Standard Model the sine term of the time dependent CP asymmetry in this channel is suppressed respect to $\sin 2\beta$, being proportional to a factor related to the helicity suppression of left-handed respect to right-handed photons. This measurement, which is sensitive to New Physics couplings with the opposite helicity, will continue to be statistics limited up to 50 $ab^{-1}$. An alternative method of studying the photon polarization in $b \to s\gamma$ is the Dalitz plot distribution of the $K\pi\pi$ system in $B^0 \to K\pi\pi\gamma$, but this also requires a large statistics sample.

### 4.1. Rare Decay Branching Fractions

Many rare $B$ decay modes can potentially give access to physics beyond the Standard Model via measurements other than of *CP*-violating asymmetries. Some examples of these modes are listed in Table III. Typically, these decays do not occur at tree level and consequently the rates are strongly suppressed in the Standard Model. Substantial enhancements in the rates and/or variations in angular distributions of final state particles could result from the presence of new heavy particles in loop diagrams, resulting in clear evidence of New Physics. Moreover, because the pattern of observable effects in highly model-dependent, measurements of several rare decay modes can provide information regarding the source of the New Physics.

The ratio of $b \to d\gamma$ to $b \to s\gamma$ decays is directly related to the ratio $V_{td}/V_{ts}$. It is interesting to measure this ratio in penguin processes as well as through $B_d/B_s$ mixing, since New Physics enters in different ways. The ratio of the exclusive decays $B \to \rho\gamma$ and $B \to K^*\gamma$ can be accurately measured, but the precision of the determination of $V_{td}/V_{ts}$ is limited by theoretical uncertainties of $\approx 12\%$ in the ratio of the form factors. A measurement of the ratio of the inclusive decays does not suffer from this uncertainty, but is experimentally rather challenging, and requires a large data sample.

Searches for $B \to s\nu\bar{\nu}$, either inclusively or exclusively, are extremely difficult, due to the presence of the two final state neutrinos. The required sensitivity can, however, be obtained using the recoil method, in which the signal mode (in this case the exclusive $B \to K\nu\bar{\nu}$ and $K^*\nu\bar{\nu}$ modes) is sought in the recoil against a fully reconstructed hadronic $B$ decay. Assuming Standard Model branching fractions, extrapolation of current analyses suggest that we would expect a signal of 10 events in each of the four modes ($K^{-,0}$, $K^{*-,0}$) although with a substantial background, with 3 $ab^{-1}$ of data. A statistically significant signal would emerge in the combination of modes with approximately 10 $ab^{-1}$ even using a simple cut-and-count analysis.

The decays $B_d \to \ell\ell$ ($\ell = e, \mu, \tau$) are somewhat less promising in the sense that it appears impossible to reach the predicted Standard Model branching fractions even with more than 50 $ab^{-1}$ of data. Moreover, $B_d \to \mu\mu$ is expected to be accessible at both LHC*b* and *B*TeV, and these experiments will also be able to access $B_s \to \mu\mu$, which is expected to provide a more stringent test of New Physics. However, even 10 $ab^{-1}$ of data will improve the existing limits on these modes by an order of magnitude, and an $e^+e^-$ $B$ Factory does have the advantage of also being able to search for $B_d \to e^+e^-$ and the (extremely challenging) $B_d \to \tau^+\tau^-$ mode.

### 4.2. $s\ell^+\ell^-$, $K\ell^+\ell^-$, $K^*\ell^+\ell^-$ Decays

The exclusive $K^{(*)}\ell^+\ell^-$ and inclusive $s\ell^+\ell^-$ decays have been intensively studied theoretically, as they provide a potentially unique window on New Physics. For example, in the Standard Model, the forward/backward asymmetry $A_{FB}$ of the lepton pair has a zero at lepton pair mass $\hat{s}_0 = 0.14$ GeV. In extensions of the Standard Model, this zero may be approached from the opposite direction, or may be altogether absent. This region of lepton pair invariant mass represents only a small fraction of the allowed kinematic region of these rare decays, so a large data sample is required to make this measurement. The measurement of $A_{FB}$ can be done at hadronic experiments, but only in the exclusive modes involving muons. Theoretical predictions are typically more precise for inclusive processes, which can only be measured at a Super $B$ Factory. It is very important to compare $A_{FB}$ in muon and electron modes, as this asymmetry can be changed by the presence of a charged Higgs. Table IV summarizes the achievable measurement precision.

## 5. EXTRAPOLATION TO 50$ab^{-1}$

The current experimental facilities are supposed to integrate a combined luminosity of $\sim 2ab^{-1}$, which will improve the present knowledge of SM related quantities and will allow more stringent bounds on New Physics (NP) parameters. Never the less, the precision will not be enough to significatively determine the values of such parameters, even in the optimistic scenario of an early discovery of NP at LHC. A

TABLE II: Measurement precision for *CP* asymmetries in rare decays sensitive to New Physics.

| ***CPV* in Rare Decays** | | **$e^+e^-$ Precision** | | |
|---|---|---|---|---|
| **Measurement** | **Goal** | **3/ab** | **10/ab** | **50/ab** |
| $S(B^0 \to \phi K_S^0)$ | $\approx 5\%$ | 16% | 8.7% | 3.9% |
| $S(B^0 \to \eta' K_S^0)$ | $\approx 5\%$ | 5.7% | 3% | 1% |
| $S(B^0 \to K_S^0 \pi^0)$ | | 8.2% | 5% | 4% |
| $S(B^0 \to K_S^0 \pi^0 \gamma)$ | SM: $\approx 2\%$ | 11% | 6% | 4% |
| $A_{CP}(b \to s\gamma)$ | SM: $\approx 0.5\%$ | 1.0% | 0.5% | 0.5% |
| $A_{CP}(B \to K^*\gamma)$ | SM: $\approx 0.5\%$ | 0.6% | 0.3% | 0.3% |

TABLE III: Measurement precision for rare decays sensitive to New Physics.

| **Rare Decays** | | **$e^+e^-$ Precision** | | |
|---|---|---|---|---|
| **Measurement** | **Goal** | **3/ab** | **10/ab** | **50/ab** |
| $\lvert V_{td}\rvert/\lvert V_{ts}\rvert \sim \sqrt{\frac{\mathcal{B}(b\to d\gamma)}{\mathcal{B}(b\to s\gamma)}}$ | | 19% | 12% | 5% |
| $\mathcal{B}(B \to D^*\tau\nu)$ | $\mathcal{B} = 8 \times 10^{-3}$ | 10% | 5.6% | 2.5% |
| $\mathcal{B}(B \to s\nu\bar{\nu})$ ($K^{-,0}, K^{*-,0}$) | 1 exclusive: $\sim 4 \times 10^{-6}$ | $\sim 1\sigma$ (per mode) | $> 2\sigma$ (per mode) | $> 4\sigma$ (per mode) |
| $\mathcal{B}(B_d \to$ invisible$)$ | | $< 2 \times 10^{-6}$ | $< 1 \times 10^{-6}$ | $< 4 \times 10^{-7}$ |
| $\mathcal{B}(B_d \to \mu\mu)$ | $\sim 8 \times 10^{-11}$ | $< 3 \times 10^{-8}$ | $< 1.6 \times 10^{-8}$ | $< 7 \times 10^{-9}$ |
| $\mathcal{B}(B_d \to \tau\tau)$ | $\sim 1 \times 10^{-8}$ | $< 10^{-3}$ | $O(10^{-4})$ | ? |
| $\mathcal{B}(\tau \to \mu\gamma)$ | | | $10^{-9}$ | $10^{-9} - 10^{-10}$ |

more reasonable value for the statistics needed is $\sim 50ab^{-1}$, which can be achieved in with a data taking of the order of one year at the facility proposed in this document. With such a precision, the UT analysis will became a high precision test, as shown in fig. 8.

The plot represents the Universal Unitarity Triangle analysis [16], which is a UT fit performed using only quantities that are independent of NP contributions within MFV models. [2] This is a common starting point of the SM analysis, as well as of any study of MFV scenarios [18]. Even if this fit is obtained from the standard analysis removing those quantities that are sensitive to NP (which provides a bound on NP parameters once the UUT is given as input), we will be able to achieve a precision of the order of percent on $\bar{\rho}$ and $\bar{\eta}$. This MFV generalized analysis will be precise enough to overcome the present SM fit, shown in figure (3).

At the same time, the improvement of the measurements of $b \to s$ processes will allow to strongly bound the values of the mass insertions parameters of figure (7), as shown in figure (9). Here, we assumed the pessimistic scenario in which the two experimental inputs ($BR(b \to s\gamma)$ and $BR(b \to sll)$) will be in perfect agreement with the SM. The experimental precision, in this case, will be enough to test NP effects at the percentage level. AT the contrary, there will be enough sensibility to translate any future experimental discrepancy into useful information for the interplay between flavour physics and the direct search of NP at the hadron colliders.

Another important aspect to stress is the strong connection of $B$ and $\tau$ physics, in the framework of testing GUT models. An example of this is provided in figure (10), where the impact of the Upper Limit on $BR(\tau \to \mu\gamma)$ is shown on the same plot of figure (7), once $b \to s$ and $\tau \to \mu$ decays are connected in the framework of GUT. [19] In general, with the high luminosity that a *SuperB* factory can collect, rare decays of $\tau$ leptons can be studied with high precision, providing a stringent test of flavour violation in the leptonic sector and boosting our capability of testing GUT models.

[2] In practise, one cannot use $\epsilon_K$ and $\Delta m_d$ to determine $\bar{\rho}$ and $\bar{\eta}$ independently of NP. On the other side, after the UUT analysis is performed, these two bounds provide constraints on the scale of NP particles [8, 17].

# Part II
# Detector Working Group Report

The *BABAR* and *Belle* detectors have proven to be very effective instruments to explore precision flavor physics. The detector working group considers that their basic design remains valid at *SuperB*, provided some subsystems can be modified as discussed in the following.

The *SuperB* linear collider design employs low-current beams crossing at a frequency in the MHz range with a very small beam spot size, resulting in a relatively low machine

TABLE IV: Measurement precision for $s\ell^+\ell^-$, $K\ell^+\ell^-$, $K^*\ell^+\ell^-$ decays.

| $s\ell^+\ell^-$, $K^{(*)}\ell^+\ell^-$ Decays | $e^+e^-$ Precision | | |
|---|---|---|---|
| **Measurement** | **3/ab** | **10/ab** | **50/ab** |
| $\mathcal{B}(B \to K\mu^+\mu^-)/\mathcal{B}(B \to Ke^+e^-)$ | ~ 8% | ~ 4% | ~ 2% |
| $A_{CP}(B \to K^*\ell^+\ell^-)$ (all) | ~ 6% | ~ 3% | ~ 1.5% |
| (high mass) | ~ 12% | ~ 6% | |
| $A_{FB}(B \to K^*\ell^+\ell^-)$ : $\hat{s}_0$ | ~ 20% | ~ 9% | ~ 9% |
| : $A_{CP}$ | | | |
| $A_{FB}(B \to s\ell^+\ell^-)$ : $\hat{s}_0$ | ~ 27% | ~ 15% | ~ 7% |
| : $C_9$, $C_{10}$ | 36 – 55% | 20 – 30% | 9 – 13% |

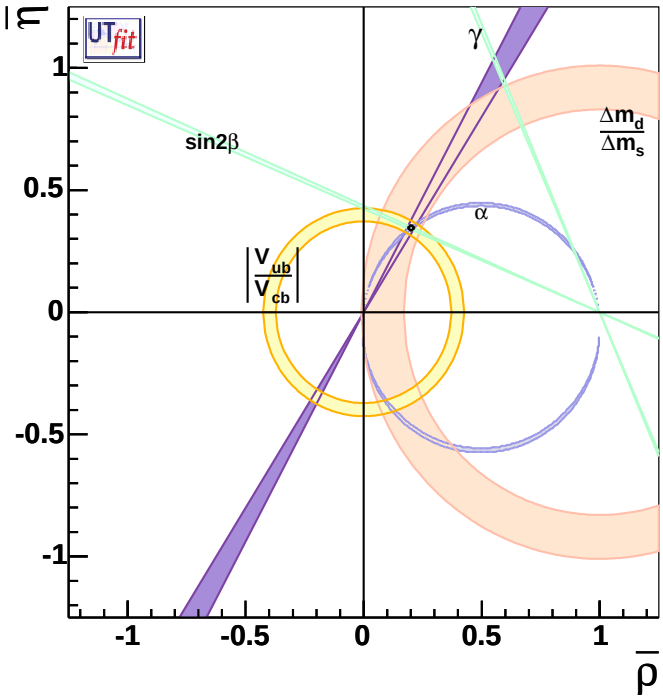


FIG. 8: Extrapolation of the Universal UT analysis to a statistics of $50ab^{-1}$.

background rate. In addition, machine design and cost argument require a reduction in the energy asymmetry changing the boost from the current $\beta\gamma = 0.56$ of *BABAR* and 0.45 of *Belle* down to 0.2 – 0.3.

Under these conditions, in particular the low background rate, many of the *BABAR* or *Belle* subsystems would be directly reusable at *SuperB*, or would require some design optimization within the same technology choice, mainly driven by the beam crossing time structure.

On the other hand the smaller boost, reducing the separation between the two $B$ decay vertices, requires an improved vertexing resolution to maintain the physics reach. This improvement is possible thanks to the small beam dimensions that allow a reduction of the beam pipe radius to 1.0 cm or less, but will require significant R&D on the detector technology needed to instrument the small radius tracking region. Particle identification will also require R&D to improve the compactness of the light detection system and extend angular coverage. Some amount of R&D will also be required to optimize crystals for small angle calorimetry, where the high Bhabha rate will increase occupancy beyond the capabilities of current CsI(Tl) systems.

In the following we discuss how machine parameters such as boost and energy spread affect the detector design and physics reach (Sec. 6), what machine and bacgkrounds are expected (Sec. 7), and the main issues for the detector subsystems (Sec. 8 – 12)

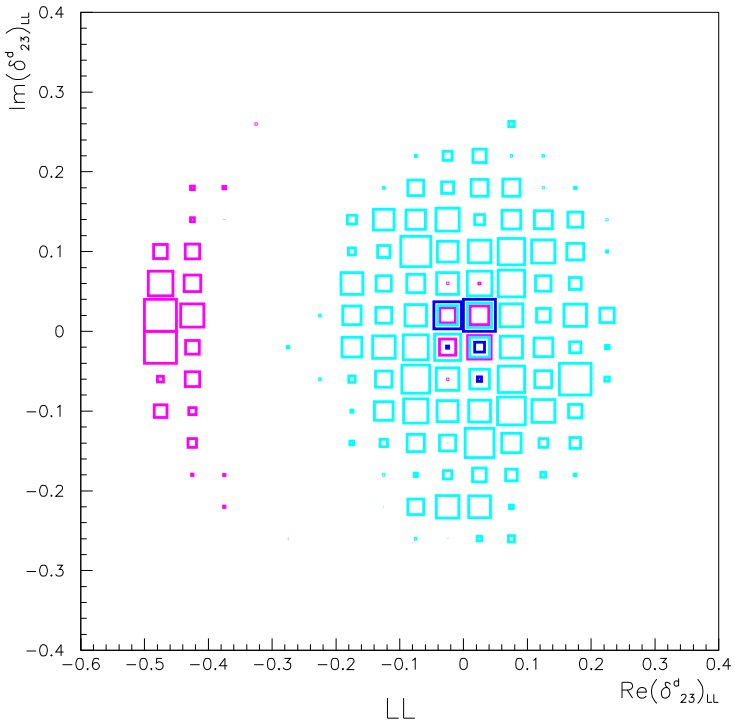


FIG. 9: Extrapolation of the the mass insertion analysis to $50ab^{-1}$: bounds from $b \to s\gamma$(violet) and $b \to sll$ (light blue) are shown, together with the combined information (dark blue).

## 6. PHYSICS DEPENDANCE ON BASIC PARAMETERS ASSUMPTIONS

There are several parameters of the *SuperB* Factory which directly impact the physics capabilities at the new accelerator. These include: the energy asymmetry or $\beta\gamma$, the center-of-mass energy spread, the beam size and beam-pipe size at the interaction point, and the probability of multiple interactions in a single crossing (or train of crossings).

The study of time-dependent *CP* violation requires that the $B^0 - \overline{B}^0$ system be boosted in the lab system, so that the $B$-meson decay vertices are separated by a measurable amount. The current $B$ Factories have boosts of $\beta\gamma = 0.56$ (PEP-II) and 0.45 (KEKB). Lower boosts are feasible with improved vertex resolution, as described below.

The $\Upsilon(4S)$ has a FWHM of roughly 18 MeV, so that the accelerator's beam energy spread will reduce the effective cross-section to $B\overline{B}$. A center-of-mass energy spread of 5 MeV (10 MeV) corresponds to a reduction of roughly 0.85 (0.67). Exclusive reconstruction of $B$-meson decays usually rely on two kinematic variables to separate the signal from continuum ($q\overline{q}$) or random combinatoric backgrounds. Typically these kinematic variables are $m_{\rm ES} = \sqrt{(E_{Beam}/2)^2 - p_B^2}$ and $\Delta E = E_B - E_{Beam}/2$, where all quantities are in the center-of-mass. The width of the $m_{\rm ES}$ distribution is determined almost exclusively by the accelerator's center-of-mass energy spread, and a larger energy spread reduces the background separation achievable with this kinematic variable. Broadening of the $m_{\rm ES}$ distribution is ultimately limited by the width of the $\Upsilon(4S)$, since the energy spread convoluted with the $\Upsilon(4S)$ line-shape is the relevant distribution. The $m_{\rm ES}$ width saturates at roughly 5.5 MeV, or a factor of two wider than PEP-II.

The much smaller beam-spots at the *SuperB* machine will permit smaller beam-pipes, allowing the first active layer of a Silicon Vertex detector to be closer to the interaction point. Such improvements will be necessary to reduce the energy asymmetry, while maintaining the ratio of $B$ vertex separation over vertex resolution at or above 2.5. In addition, such improved vertexing may allow improved flavor tagging and background rejection. For example, it may be possible to identify the charm vertex in semi-leptonic decays, to better separate leptons from $B$ as opposed to charm decays.

Lastly, the time structure at the SuperB machine will be different from that at the current $B$ factories. The bunch collision frequency will be of order 1 MHz, compared to 238 MHz at PEP-II. At this frequency, for a luminosity of $\mathcal{L} = 10^{36}$, the roughly 100 nb cross-section, for all processes, corresponds to an interaction in every tenth crossing. This implies that in about 10% of all $B\overline{B}$ events there will also be a Bhabha or two-photon interaction, and roughly 1% of

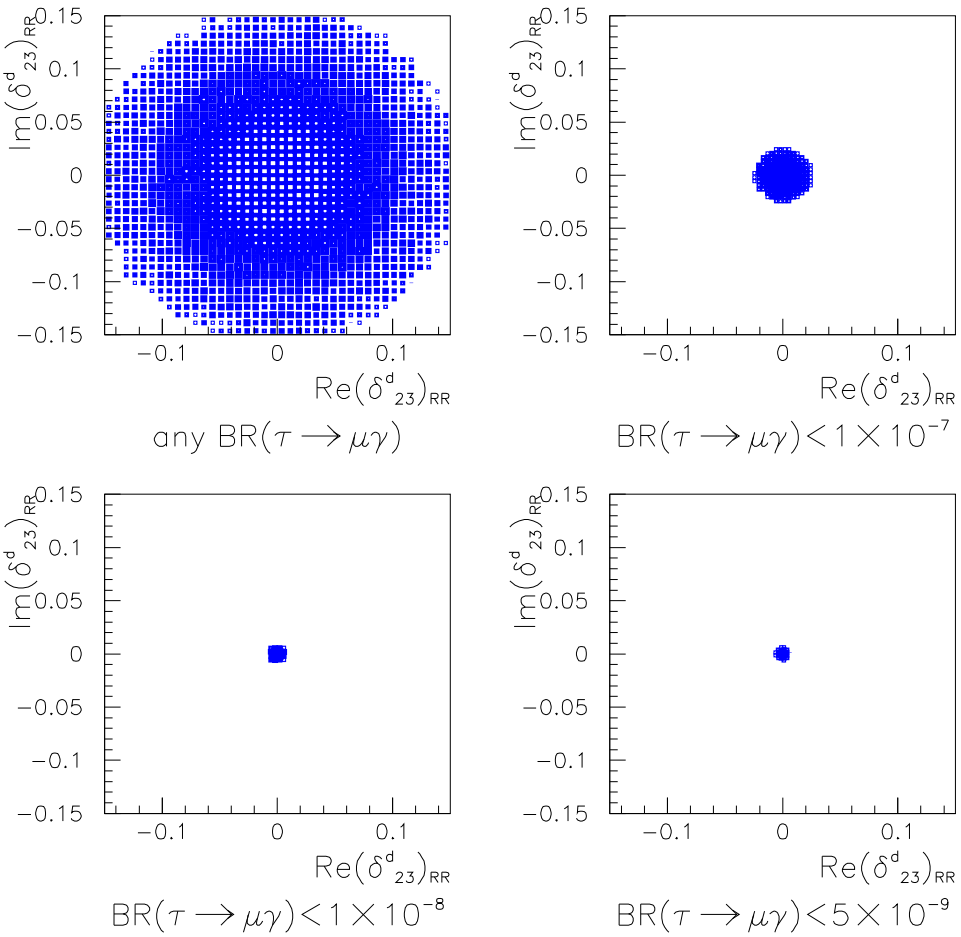


FIG. 10: Impact of the Upper Limit on $BR(\tau \to \mu\gamma)$ on the mass insertion parameters $\delta^{23}$ in GUT scenario.

the time there will be a second $q\overline{q}$ or $B\overline{B}$ event as well. This *physics pile-up* will produce additional background for rare processes, but can be removed with global event energy requirements.

## 7. MACHINE BACKGROUNDS

The reduction in beam currents in a linear-colliding *B*-Factory design, as compared with a standard storage ring configuration, results in a dramatic reduction in single-beam background (which would otherwise be the dominant background source). The single-beam background sources, for example beam-gas, should be negligible compared with the luminosity-scaling sources detailed below. A precise background prediction is not possible at this stage given the preliminary nature of the machine design. However, the detailed characterization of the various background sources on the present PEP-II and KEK-*B* machines, as well as experience from SLC and studies for backgrounds at the ILC, allow us to extrapolate the background sources which are important for consideration at present:

**Luminosity Sources** The most dangerous background source is radiative Bhabha debris. In this case, the background rate is strictly proportional to luminosity and therefore will be 100 times higher at a Super *B* Factory than today. To control this source, magnetic bending elements should be kept as far as is practical from the interaction point in order to prevent off-momentum electrons or positrons from reaching apertures close to the detector. At PEP-II, the presence of a strong dipole field only 20 cm away from the IP, required to separate the two beams in the absence of a crossing angle, accounts for the fact that this background is quite prominent while being small or negligible at KEK-*B*. At *SuperB*, the

first magnetic elements will be focusing quadrupoles located approximately 40 cm away from the IP. Due to the lack of nearby dipoles, the "luminosity" background should be substantially reduced from a simple extrapolation from PEP-II, but potentially larger than indicated by the KEK-*B* extrapolation. We have assumed, as a baseline, a factor 5 reduction with respect to the PEP-II extrapolation, but subdetectors have considered the full range between 0.2 and 1 times the PEP-II-based extrapolation as a measure of the uncertainty in the estimates.

**Beam-beam interactions.** Beam-beam interactions, *i.e.,* the transverse blowup of one beam due to its interaction with the other, will be one major source of particle loss rate. Backgrounds will be produced by beam tails which are created by this mechanism and then hit nearby apertures. Quantitative prediction of these tails is almost impossible, especially when the machine is operated close to its limits where they tend to get very large. The best means to control the contribution is to design an advanced collimator scheme that can prevent beam tails from hitting apertures near the detector. The detector must also be well protected against the secondaries produced at the collimators. The maximum amount of collimation will be determined by the lifetime loss observed when closing the collimators. It is therefore prudent to integrate the collimator design as early as possible into the machine design to have control of this background source. The observed PEP-II beam-beam terms have been roughly parameterized and extrapolated, leading to a conclusion that this source will make a negligible contribution. However, it will require a very substantial effort to realize such performance at *SuperB*.

**Touschek background.** Touschek background, *i.e.,* longitudinal beam blowup due to intrabunch scattering, will be present and is proportional to the bunch density. It will therefore be significantly increased with respect to the present PEP-II value. This effect accounts for a significant part of the *Belle* background (around 20%) but is barely visible in PEP-II. Its effect on the detector will again be a very sensitive function of the magnetic elements in that area. This background can be modeled in principle rather well and a good extrapolation should be available in the coming months.

**Synchrotron radiation.** As noted above, we expect the *single-beam* sources of synchrotron radiation to be negligible, due to the low beam currents. The amount of *beam-beam* synchtrotron radiation ("beamstrahlung") should be greater than either the present *B*-Factories or in a super-*B* configuration using a standard storage ring; however it should be small compared with, for example, the ILC, or even the SLC, due to the much lower beam energies. A 5 $\mu$m gold masking similar to that presently within the PEP-II beampipe should be sufficient to remove this contribution (and may perhaps be able to be made even thinner).

All subdetectors are required to satisfy a factor of five safety margin to take into account for these extra terms. A large safety margin is also needed to cope with background fluctuations.

To guarantee high operational efficiency, it is essential that the detector can stand short background bursts, of magnitude comparable with the steady level. Such bursts, typically lasting a few seconds, are seen very frequently (up to 1 per hour at KEK-B) and are attributed to dust particles attracted from the beam pipe to the center of the beam. This implies detectors with large safety margins in terms of integrated dose and radiation bursts.

Finally, proper instrumentation must be integrated from the start into the detector and machine designs, in order to measure the background, isolate its various sources and monitor its evolution in a continuous fashion.

In conclusion, although backgrounds are expected to be significantly smaller at a linearly-colliding *B*-Factory than in a configuration using a standard storage ring, they are still of crucial import in the design of the detector and interaction region to minimize the sources of backgrounds that are not reduced by a reduction in single beam currents. In particular, the design of the IR to minimize radiative-Bhabha background, and the ability of detector elements to withstand short background bursts, are both of critical importance.

## 8. VERTEXING

The *SuperB* interaction region design is characterized by the small size of the transversal section of the beams, fraction of $\mu$m for $\sigma_x$ and tens of nm for $\sigma_y$. Therefore it will be possible to reduce the radial dimension of the beam-pipe tube up to $5-10$ mm radius, still preventing the beams to scatter into the tube within the detector coverage angle. The Be thickness of the tube will be reduced down to $200-300\,\mu$m, corresponding to $(5.6-8.5)\cdot 10^{-4}X_0$, depending on the value of the radius of the beam pipe. Another feature of the innovative SuperB design is the low current circulating inside the beam-pipe, tens of mA, in spite of the high luminosity. The cooling system for the beam-pipe will be not necessary and it has been removed in the design. The reduced amount of radial material and the possibility to measure the first hit of the track very close to the production vertex will benefit the track parameters determination.

First Monte Carlo studies indicate precise determination of the $B$ decay vertices at the level of $10-20\,\mu$m and consequently on the $\Delta z$ separation along the beam axis among the two $B$ mesons, basic ingredients for the time dependent analysises.

The multiple scattering contribution to the resolution on the decay vertex is no more dominating since the amount of radial material is very much reduced with respect to the B-factory scenario. The intrinsic spatial resolution fixed

by the pitch width of the silicon vertex detector will add a non-negligible contribution on the vertex measurements and therefore it will be important to minimize it as much as possible in a future vertex detector.

For the simulation study we added a 50 $\mu$m Monolithic Active Pixel silicon layer, in addition to the current *BABAR* silicon vertex detector, mounted on a 50 $\mu$m kapton foil and glued directly on the beam-pipe. This configuration allows to measure the first hit of the track just outside the beam-pipe. In figure 11it is shown the resolution on the proper time difference of the two $B$ ($\Delta t$) for three different beam-pipe configurations:

- 0.5 cm radius: consider this as the aggressive scenario where we can evaluate the very limit of the vertex resolution we can think to achieve. We considered 200 $\mu$m Be thickness for the beam-pipe and 5 $\mu$m spatial resolution on hits from charged tracks.
- 1.0 cm radius: most likely scenario with 300 $\mu$m Be thickness for the beam-pipe and 10 $\mu$m spatial resolution on hits from charged tracks.
- 1.5 cm radius: conservative scenario with 500 $\mu$m Be thickness and 10 $\mu$m spatial resolution on hits from charged tracks.

In all the configuration we have considered a $5-\mu$m-thick gold foil (equivalent to 150 $\mu$m of silicon) before the first layer of the vertex detector in order to absorb low energy background photons.

The spectacular precision of the decay vertex determination will also benefit several aspects of the $B$ meson reconstruction. The possibility to reduce the energy asymmetry without affecting the proper time resolution will enlarge the acceptance of the detector improving the reconstruction of decay modes with neutrinos ($B \to \tau\nu$, $B \to D^{(*)}\tau\nu$, $\tau$ decays, etc.). The ability to separate the $B$ from the $D$ vertex would help rejecting the $q\bar{q}$ events ($q = u, d, s, c$ quarks) and would open new analyses techniques for $B$ flavor tagging based on topological algorithms. This possibility has still to be quantitatively estimated.

## 9. TRACKING

Charged particle tracking is performed at *BABAR* and *Belle* through a combination of silicon strip detectors and drift chamber. This design allows a high resolution determination of the track parameters near the interaction point while retaining good momentum resolution in the gaseous drift chamber. Occupancies in the two systems are acceptable with background currently experienced at the two $B$ Factories and we expect that a similar detector design will be usable at *SuperB*.

A small radius vertexing device, directly mounted on the beam pipe, will be required to improve vertex resolution. Monolithic active pixel systems are being developed by several groups and are a very promising technology for this application. In these devices the active detection thickness is only of the order of 10-20 $\mu$m, and they can therefore be thinned down to 50 $\mu$m, thus significantly recucing the amount of material in the first detection layer.

The current silicon strip detector systems have four or five layers, strip lengths between 5 and 20 cm, strip pitch between 50 and 200 $\mu$m, and are readout through preamplifiers with shaping times between 100 and 400 ns. Given the time structure of events at *SuperB* and the projected low backgrounds, it should be possible to increase the shaping time of the preamplifiers to 0.5-1 $\mu$s, thus improving the signal to noise ratio and making it possible to reduce the detector thickness from the current 300 $\mu$m to 200 $\mu$m.

If the amount of material is reduced, decreasing the intrinsic resolution from the current 12-20 $\mu$m to 5-10 $\mu$m through a finer pitch readout would both benefit the momentum resolution, especially for high momentum particles, and improve the angle measurement, which is crucial for vertexing as well as for particle identification based on Čerenkov angle determination. The small angle region will require special attention because of the high rate Bhabha scattering. Depending on the specific choice of boost and angular coverage a special section of silicon strips with finer segmentation and/or shorter shaping time will be required. This section could be organized in forward and backward disks or cones electrically separated from the central part of the detector.

The *BABAR* and *Belle* drift chambers are conceptually similar but have different dimensions: from 23.6 to 80.9 cm for *BABAR*; from 16 to 114 cm for *Belle*. They use He-based gas mixtures, with cell sizes from 12 to 18mm. Maximum drift time is around 500 ns and the resolution about 100 $\mu$m in the best part of the cell. In preparation for luminosity upgrades, *Belle* has experimented with small cell (5.4 mm) drift chamber for the inner layers of the CDC finding a significant rate reduction but a deteriorated resolution (150 $\mu$m).

We expect that the reduction in cell size will not be needed at *SuperB*. On the contrary one could take advantage of the time structure of the events and increase the drift time to up to 1 $\mu$s with the intent of improving the resolution. A full optimization of the drift chamber design will only be possible when detailed background simulations are available.

## 10. PARTICLE IDENTIFICATION

Particle identification is a central aspect of the criteria describing the desired properties of a detector working at *SuperB*. Such a detector system generally requires good tracking information to help optimize the PID function, good start time information and generally needs supplementary information, (such as $dE/dx$ from the energy loss from the tracking chambers), to cover the full desired momentum range.

The *BABAR* and *Belle* detectors incorporate relatively complete PID systems, which essentially provide the needed performance for their respective environments. The *BABAR* DIRC system has been particularly robust, relatively insensitive to background, covers most of the momentum range

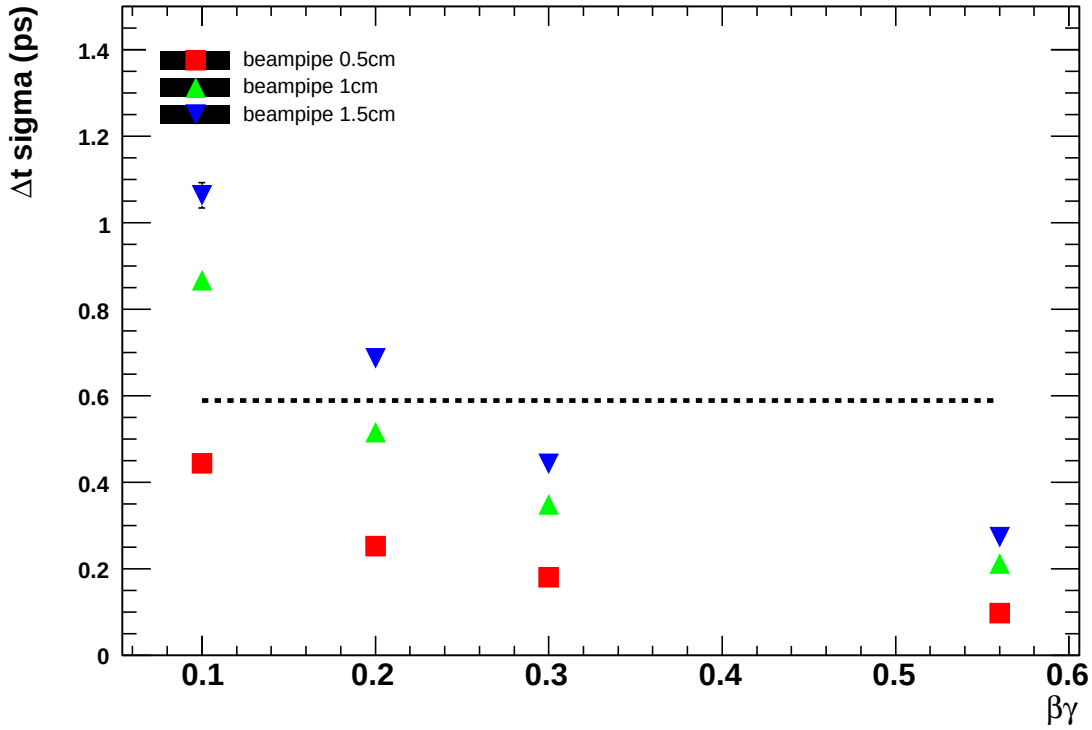


FIG. 11: $\Delta t$ resolution as a function of the $\beta\gamma$ boost value of the center of mass rest frame for different beam-pipe configutions: 0.5 cm, 1.0 cm and 1.5 cm radius. The dashed line represents the *BABAR* reference value.

for all particle species, and has extremely good misidentification properties. A new PID system based on the DIRC technique but using modern photon detectors, such as a Fast Focusing DIRC or a TOP, would provide more complete geometrical and momentum coverage, and perhaps better rejection at the highest momenta. The final choice of collision energies at the SuperB Factory will define the highest energy/momentum needed for pion/kaon separation. It is also probable that the End Cap regions will require more attention than has been given for the current detectors.

The environment at the proposed SuperB Factory should not be a problem for the PID systems described above. The beam currents are down a lot, and the backgrounds should be much less severe than presently experienced, although this will depend, in detail, on the design and implementation of the final focus system The data acquisition problem will be interesting, but quite manageable, requiring a pipelined approach, but similar to the solution for other systems, and achievable with commodity equipment.

More generally, the technologies of choice for PID in a new super B factory detector appear to be two variations of the Čerenkov focusing device, either in two or in three dimensions the DIRC of BaBar, a fast DIRC, or the TOP of *Belle*; and two systems that have special interest for the end cap regions an aerogel proximity focusing device, and possibly conventional time of flight with really good timing, (of order 30 picoseconds) providing there is adequate momentum resolution from the forward tracking devices.

Any new technology proposed to replace the established PID systems will require a thorough and aggressive R&D activity, proving not only the device particle identification performance in real life conditions, but also to demonstrate the photon detector lifetimes, robustness and reliability, under realistic conditions.

The SLAC group is in the middle of beam test of the Fast Focusing Dirc idea, with encouraging results. We are also in the middle of testing the micro-channel plate single photon detectors in magnetic fields up to 15 KGauss, with encouraging results.

## 11. CALORIMETRY

Although detailed background calculations for *SuperB* have not yet been done, the existing CsI(Tl) electromagnetic calorimeters of *BABAR* and *Belle* should be suitable for use at the *SuperB* MegaHertz collision rate, at least for the main barrel sections. The long (1.3 $\mu$s) decay time of CsI(Tl) should not be a severe problem. The radiation dose rate should be an order of magnitude smaller than at the current

*B* factories. The barrel calorimeters of either current detector should therefore be adequate without modification.

There may, however, be reason to consider upgrading the endcap calorimeters. It is likely that the smaller size of beamline elements inside the detector will allow extension of the solid angle coverage for tracking and calorimetry. This would be beneficial to all rare decay physics involving missing energy, including such important topics as as measurement of $B \to \tau\nu$ or $B \to K\nu\bar{\nu}$ branching fractions.

The cross section for Bhabha scattering events at 100 mrad in the endcap region is more than an order of magnitude greater that it is at 300 mrad; at small polar angles there will thus be a significant number of events in which a Bhabha electron overlaps a hadronic event. The most effective way to combat this is to use a photon detection medium with faster response and shorter Molière radius, to minimize the probability of temporal or spatial overlaps. Development work on suitable crystals, cerium-doped lutetium orthosilicate (LSO) and lutetium yttrium orthosilicate (LYSO), which have a Molère radius 60% of that of CsI, is underway at Caltech. The two crystals are very similar, with LYSO somewhat easier to grow and thus somewhat less expensive. LSO/LYSO is also mechanically strong, and is not hygroscopic. A comparison of the properties of CsI(Tl) and LSO/LYSO(Ce) is shown in Table V.

A replacement of the existing endcaps in *Belle* or replacement of the existing forward endcap in *BABAR* and the addition of a rear endcap is thus likely to be a worthwhile upgrade. This would allow extension of the solid angle coverage to the 100 mrad regime, and minimize the number of events with overlapping Bhabhas. The *BABAR* forward endcap calorimeter covers the solid angle down to 350 mrad; there is no backward endcap. The forward calorimeter of *Belle* covers the region down to 200 mrad, while the backward endcap calorimeter extends to 400 mrad.

The spectrum of scintillation light in LSO(Ce) peaks at 420 nm, has a total light output 65% of that of CsI(Tl), a very fast decay time of 42 ns and is extremely radiation hard. The spectrum is well-matched to solid state readout by an avalanche photodiode (APD) or a conventional photodiode. A $^{137}$Cs spectrum using a full-size LSO bar and a single Hamamatsu APD, as well as comparison to a photomultiplier tube, is shown in Figure 12.

A certain amount of additional R&D is necessary to bring LSO/LYSO(Ce) to a state in which one could build an actual calorimeter. This R&D involves optimization of the uniformity of the cerium dopant, analysis and removal of trace impurities from the basic salt, which are the source of a small amount of phosphorescence observed under intense radiation doses, and further optimization of the APD readout. There is already enough crystal growth capacity to produce the endcap crystals in a few months. Working with the crystal growers, we expect to be able to resolve the remaining large crystal-related issues and to bring the price into a more affordable range. These tasks could all be accomplished within a year or two; an LSO(Ce) upgrade of the endcap regions of either *BABAR* or *Belle* could thus be accomplished on the desired time scale.

### 12. MUON DETECTOR

The muon detection system at current *B* Factories is realized by instrumenting the flux return yoke of the magnets with large area tracking detectors made of resistive plate chambers or limited streamer tubes. These technologies have limited rate capabilities, but with the current understanding of machine backgrounds it will be possible to use these detectors at *SuperB*. Special care must be taken to shield the outermost layers of the muon detection systems from radiation coming from the tunnel. This could be generated for instance by synchrotron radiation backsplashing on far-away masking elements. In addition, depending on the choices on the boost and on the minimum angular coverage, the small angle portion of the detector will probably require increased segmentation of the readout and/or separate gas volumes. There seem to be no significant technological problem in designing the muon detection system at *SuperB*.

### 13. TRIGGER-DAQ

The trigger and DAQ system for the detector at the SuperB Factory will have the task of handling the large event and data rates produced at a luminosity of $\mathcal{L} = 10^{36}$. The type of trigger needed depends critically on the bunch collision frequency. At frequencies at or below 1 MHz an online trigger would only provide a factor of 10 or less in rejection, and at this level all event rejection could be implemented instead in software triggers. At frequencies above 1 MHz a hardware trigger would be desirable to reduce the event readout rate to the 100 kHz level. For any configuration, highly pipelined readout in the DAQ system will be necessary. Any detector operating at $\mathcal{L} = 10^{36}$ will have DAQ rates of the order of 5 GBytes/sec. This high rate is, however, roughly an order of magnitude smaller than the front-end read-out rates of the LHC experiments. Extrapolations, including Moore's law scaling for networks, disks, and CPUs, indicate that the trigger and DAQ at SuperB will be comparable in difficulty to the current *BABAR* system.

# Part III
# Initial Parameters for a Linear Super-B-Factory

A Super B Factory, an asymmetric energy $e^+e^-$ collider with a luminosity of order $10^{36}$ cm$^{-2}$s$^{-1}$, can provide a sensitive probe of new physics in the flavor sector of the Standard Model. The success of the PEP-II and KEKB asymmetric colliders [20, 21] in producing unprecedented luminosity above $10^{34}$ cm$^{-2}$s$^{-1}$has taught us about the acceler-

TABLE V: Comparison of the properties of CsI(Tl) and LSO/LYSO(Ce)

| | CsI(Tl) | LSO/LYSO(Ce) |
|---|---|---|
| Radiation length (cm) | 1.85 | 1.14 |
| Molière radius (cm) | 3.5 | 2.3 |
| Peak luminescence (nm) | 560 | 420 |
| Decay time (ns) | 1300 | 42 |
| Relative light yield | 1 | .65 |

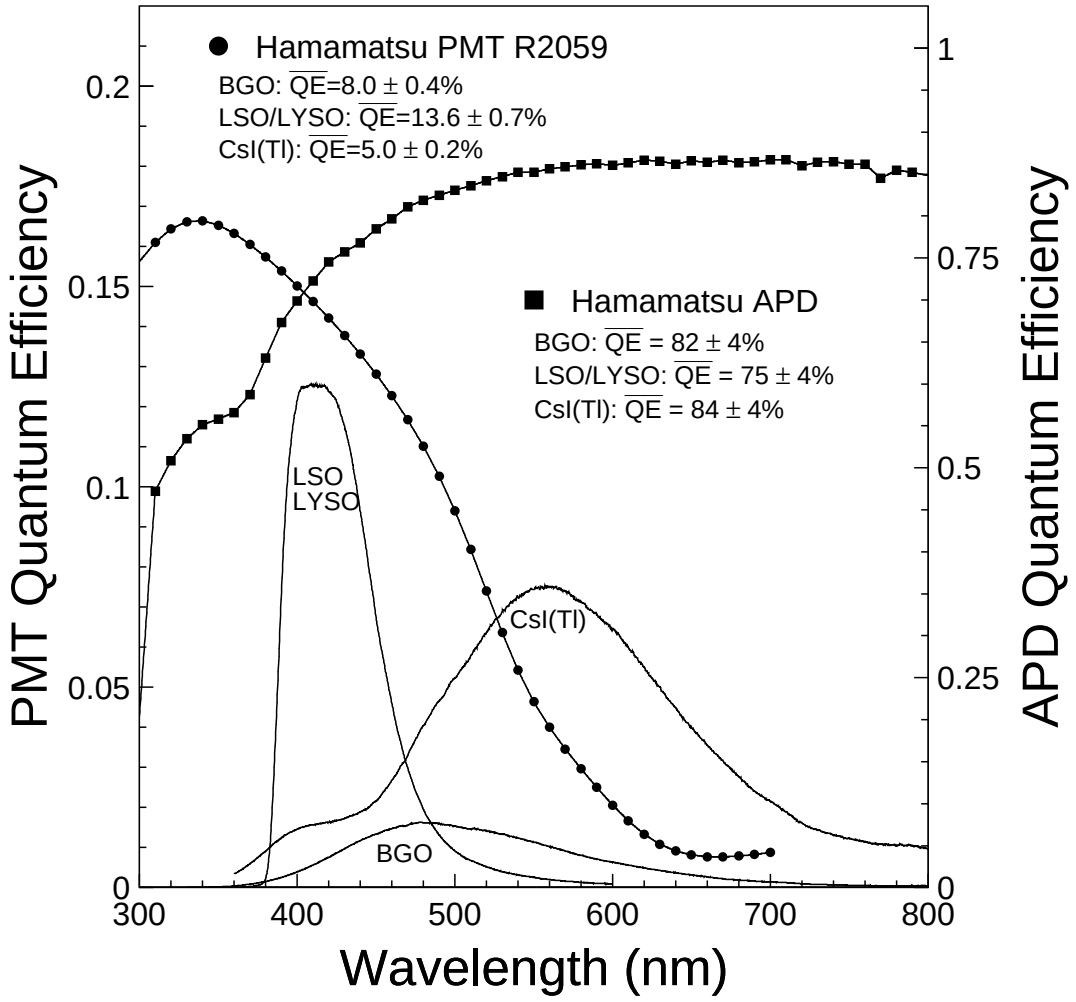


FIG. 12: Emission spectra of BGO, LSO/LYSO(Ce) and CsI(Tl) together with the quantum efficiency of a Hamamatsu photomultiplier tube and avalanche photodiode. The quantum efficiency averaged over the LSO/LYSO spectrum is 75% for the APD and 13.6% for the PMT.

ator physics of asymmetric $e^+e^-$ colliders in a new parameter regime. Furthermore, the success of the SLAC Linear Collider [22] and the subsequent work on the International Linear Collider [23] allow a new Super-B collider to also incorporate linear collider techniques. This note describes the initial parameters of a linearly colliding asymmetric B-Factory collider at a luminosity of order $10^{36}$ cm$^{-2}$s$^{-1}$. Such a collider would produce an integrated luminosity of about 10,000 fb$^{-1}$ (10 ab$^{-1}$) in a running year ($10^7$ sec). Design studies are continuing to improve these parameters.

## 14. DESIGN FROM PAST SUCCESSES

The construction and operation of modern multi-bunch $e^+e^-$ colliders have brought about many advances in accelerator physics in the area of high currents, complex interaction regions, high beam-beam tune shifts, high power RF systems, controlled beam instabilities, rapid injection rates, and reliable uptimes ($\sim$ 95%).

The present successful B-Factories have proven that their design concepts are valid:

1. Colliders with asymmetric energies can work.

2. Beam-beam energy transparency conditions are weak.

3. Interaction regions with two energies can work.

4. IR backgrounds can be handled successfully.

5. High current RF systems can be operated (3 A×1.8 A).

6. Beam-beam parameters can reach 0.06 to 0.09.

7. Injection rates are good and continuous injection is done in production.

8. The electron cloud effect (ECI) can be managed.

9. Bunch-by-bunch feedbacks at the 4 nsec spacing work well.

Lessons learned from linear collider studies have also shown new successful concepts:

1. Bunch energy and energy spread compensation of multiple bunches in a high power linac can be done.

2. Small horizontal and vertical emittances can be produced in a damping ring with a short damping time.

3. Superconducting linacs can be used with short high-charge bunches.

4. Superconducting linacs can be used for beam energy recovery.

5. Transverse beam kickers with fast switching times and excellent stability can be produced.

6. Bunch length compression can be successfully performed.

All of the above techniques will be incorporated in the design of a future linear Super-B Factory collider.

## 15. DESIGN STATUS

The concept of combining linear and circular collider ideas to make a linear-circular B-Factory was discussed in the late 1980's, although only circular B-Factories were built in the 1990's. Recent advances in B-Factory performance and solid linear collider design progress has reopened this design avenue.

The design presented here is very recent and on-going. There are new ideas emerging on the weekly time scale and some time will be needed to allow these new ideas to be incorporated into the ultimate design. The parameters presented here are preliminary but with the intent to be self-consistent.

## 16. LUMINOSITY

The design of a $10^{36}$ cm$^{-2}$s$^{-1}$ $e^+e^-$ collider combines extensions of the design of the present $B$ Factories and linear collider concepts to allow improved beam parameters to be achieved. The luminosity L in an $e^+e^-$ collider is given by the expression

$$L = \frac{N^+N^-n_b f_c H_d}{4\pi\sigma_x\sigma_y}$$
$$\sigma = \sqrt{\beta\epsilon}$$

where $n_b$ is the number of bunches, $f_c$ is the frequency of collision of each bunch, $N$ is the number of particles in the positron (+) and electron (−) bunches, $H_d$ is the disruption enhancement factor from the collisions, $\sigma$ is the beam size in the horizontal ($x$) and vertical ($y$) directions, $\epsilon$ is the beam emittance and $\beta$ is the beta function (cm) at the collision point for each plane.

## 17. COLLIDER CONCEPTS AND LAYOUT

Schematic drawings of a Linear Super-B Factory are shown in Figure 13 and 14. The operation is described here. A positron bunch from a 2 GeV damping ring is extracted and accelerated to 7 GeV in a superconducting (SC) linac. Simultaneously, an electron bunch is generated in a gun and accelerated in a separate SC linac to 4 GeV. The two bunches are prepared to collide in a transport line where the bunch lengths are shortened. These bunches are focused to a small spot at the collisions point and made to collide. The spent beams are returned to their respective linacs with transport lines where they return their energies to the SC accelerator. The 2 GeV positrons are returned to the damping ring to restore the low emittances. The spent electron beam is discarded. The process is repeated with the next bunch. It is expected that each bunch will collide about 120 times each second and that there will be about 10000 bunches. Thus, the collision rate is about 1.2 MHz. A small electron linac and positron source are used to replenish lost positrons in the colliding process and natural beam lifetime. See Figure 13.

An alternative (see Figure 14) electron source is to use a 2 GeV damping ring to store and collide electrons in a similar fashion to positrons. This scheme would reduce the demands on the electron gun but increase the site AC power.

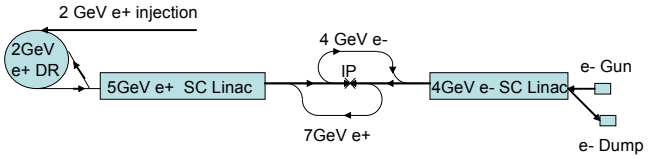


FIG. 13: Linearly colliding Super-B Factory layout

Another alternative overall design could combine the two linacs into a single unit, saving construction costs.

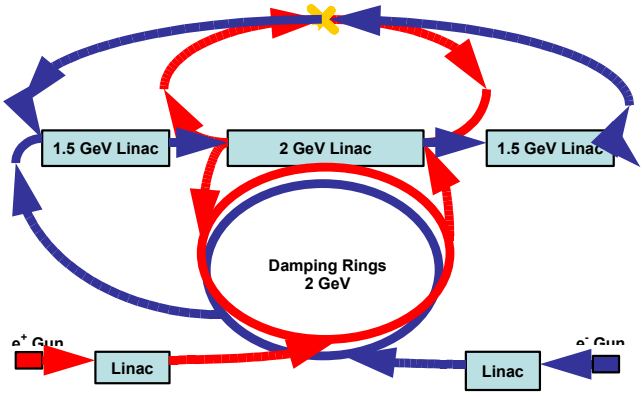


FIG. 14: Linearly colliding Super-B Factory layout

## 18. COLLISION PARAMETERS

The parameters of the beam collisions are listed in Table VI. The asymmetric energies are required to allow tracking particle vertices in the collisions.

TABLE VI: Preliminary Super-B Factory collision parameters.

| **Parameter** | **LEB** | **HEB** |
|---|---|---|
| Beam Energy (GeV) | 4 | 7 |
| Number of bunches | 10000 | 10000 |
| Collision freq/bunch (Hz) | 120 | 120 |
| IP energy spread (MeV) | 5 | 7 |
| Particles /bunch $\times 10^{10}$ | 10 | 10 |
| Time between collisions (msec) | 8.3 | 8.3 |
| by* (mm) | 0.5 | 0.5 |
| bx* (mm) | 22 | 22 |
| Emittance (x/y) (nm) | 0.7/0.0016 | 0.7/0.0016 |
| sz (mm) | 0.35 | 0.35 |
| Lumi enchancement Hd | 1.07 | 1.07 |
| Crossing angle(mrad) | 0 | 0 |
| IP Horiz. size (mm) | 4 | 4 |
| IP Vert. size (mm) | 0.028 | 0.028 |
| Horizontal disruption | 1.7 | 0.9 |
| Vertical disruption | 244 | 127 |
| Luminosity (x1034/cm2/s) | 100 | 100 |

## 19. BEAM-BEAM CALCULATIONS

The beam-beam interaction in a linear collider is basically the same Coulomb interaction as in a storage ring collider, with extremely high charge densities at IP, leading to very intense fields; since in this case quantum behavior becomes important it is necessary to use a beam-beam code to predict luminosities and related backgrounds. The "classical" effects of the beam-beam interaction are characterized by a parameter called "disruption", which can be seen as the equivalent to what the linear beam-beam tune shift is in storage rings. Typical values for D in the vertical plane are less than 30 in ILC, and more than 50 in a "linearly colliding" SuperB-Factory. The horizontal Ds are kept near or below 1 to reduce energy spread in the beam. The beam-beam interaction in such a regime can be highly non linear and unstable, leading to loss of luminosity, rather than gain, and to emittance blow-up. Since the beams must be recovered in this scheme, emittance blow-up should be kept at minimum in order to decrease the number of damping time necessary before the beams can collide again.

Let's now recall some of the scaling laws that can help in the choice of the collision parameters.

The beam-beam disruption is defined as:

$$D^{\pm}_{x,y} = \frac{N^{\mp}\sigma^{\mp}_{z}}{\gamma^{\pm}\sigma^{\mp}_{x,y}\left(\sigma^{\mp}_{x}+\sigma^{\mp}_{y}\right)}$$

where $N$ is the number of particles in one bunch, $\sigma_z$ is the bunch length, $\gamma$ is the beam energy in terms of electron mass, $\sigma_x$ and $\sigma_y$ are the beam spot sizes at collision. All the quantities refer to the opposite beam, except for the beam energy factor.

On the other hand the luminosity is proportional to:

$$L \propto \frac{N^2}{\left(\sigma_x\sigma_y\right)}$$

and the center of mass (cm) energy spread during collision can be defined as:

$$\sigma^{\rm cm}_{E} \propto \frac{N^2}{(\sigma^2_x\sigma_z)} \propto \frac{D_x N}{\sigma^2_z} \propto \frac{L\sigma_y}{(\sigma_x\sigma_z)}$$

For "linearly colliding" beams a large contribution to the energy spread comes from the beam-beam interaction via the "beamstrahlung", synchrotron radiation produced during collision. Due to the high fields at the interaction the beams lose more energy and the cm energy spread increases. This is an unwanted effect, since the $\Upsilon(4S)$ is relatively narrow, so the cm energy spread should be as small as possible.

As it can be seen from the previous formulas there are conflicting requirements for the collision parameters. In fact increasing the number of particles gives higher luminosity but also higher energy spread. Also, a short bunch gives less disruption and more luminosity, since $\beta_y{}^*$ can be decreased without having hourglass effect, but produces larger cm energy spread.

The strong-strong collision regime requires a simulation, since analytical treatment is limited. Preliminary beam-beam studies have been performed with the "GuineaPig" computer code by D. Schulte (CERN) [24], which includes backgrounds calculations, pinch effect, kink instability, quantum effects, energy loss, and luminosity spectrum. This code has been intensely used for ILC studies of beam-beam performances and backgrounds.

Some time has been spent in optimizing the "simulation" parameters, such as the number of longitudinal slices, macroparticles, grid sizes, etc... versus the computing time. Then an intensive study of the luminosity as a function of number $N$, bunch length, beam spot sizes, beam emittances and energy asymmetry has been performed, while trying to keep

small the cm energy spread and the outgoing beam emittances.

Some preliminary conclusions can be drawn from the large number of runs performed with different collision parameters:

- the bunch length should be as short as possible, this allows to increase $\beta_y^*$ and luminosity, and gives less disruption;
- given the maximum storable beam current in the Damping Ring the number of bunches should be as small as possible, i.e. the number of particles/bunch should be as high as possible (see for example Fig. 2), compatibly with the increase of the cm energy spread;
- the horizontal emittance should be increased so to minimize D: in this case less time is needed to damp the spent beams. The corresponding luminosity loss can be recovered by increasing the collision frequency;
- increasing the beam aspect ratio, i.e. having very flat beams, helps to overcome the kink instability. As a result the spent beam emittances are less disrupted, $D_y$ is smaller and the cm energy spread is not affected by the interaction.

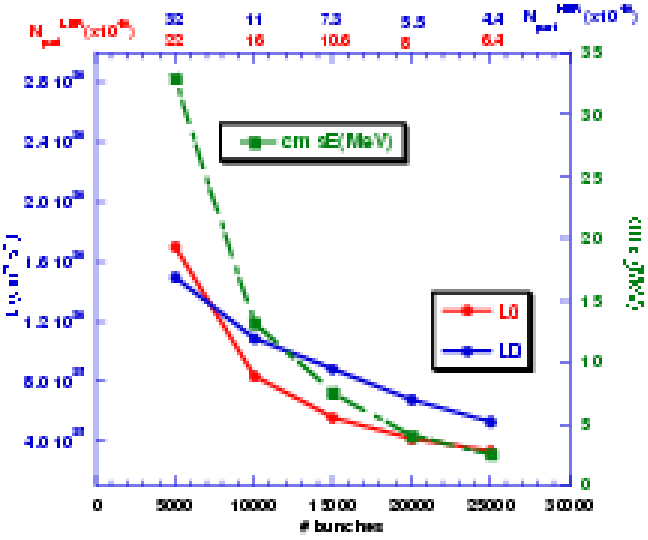


FIG. 15: Luminosity and cm energy spread vs number of bunches for fixed current in the DR. In red is the geometric luminosity, in blue the disrupted one, in green the cm energy spread in MeV.

As an example of spent beams emittances, in Figs.16 and 17 the $(x, x')$ and $(y, y')$ space phase plots after collision for both beams, with the parameters in Table VI, are shown. The different colors refer to different longitudinal bunch slices, from the bunch head to the bunch tail.

In Figs. 20 and 21 the simulated beams, before and after collision, are shown. The low energy beam is red, the high energy beam is green.

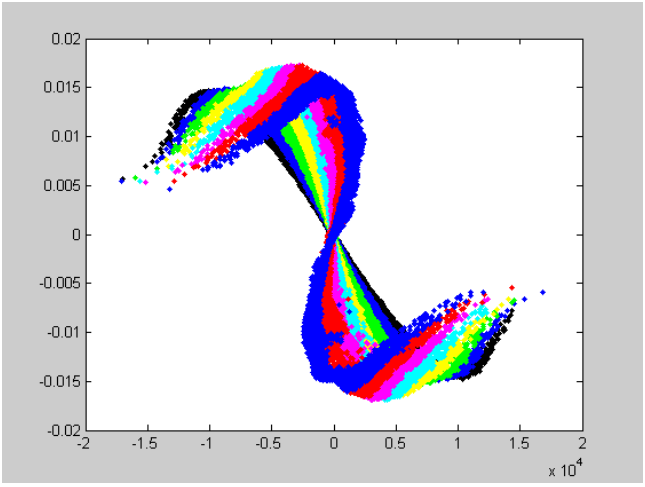

FIG. 16: Plot of the LER $(x, x')$ phase space. Each color refers to one longitudinal bunch slice.

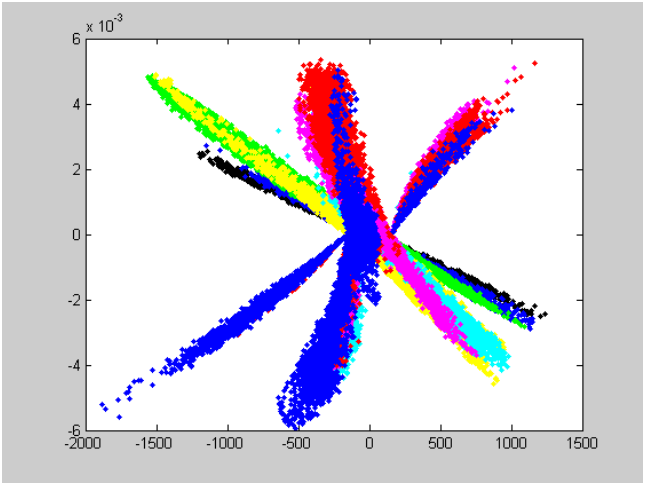

FIG. 17: Plot of the LER $(y, y')$ phase space. Each color refers to one longitudinal bunch slice.

In this particular case the disruption is very high in the vertical plane. This is what gives a large emittance blow-up. Also under study are other possibilities to reduce the emittance growth due to the collision.

The traveling focus scheme relaxes the requirements on the incoming vertical emittance together with a reduced disruption during the collision.

The four-beam DCI-like [25] beam charge compensation scheme (allowing the beams to collide again before being sent back into the Linac), it is also promising, since it could greatly reduce the disruption, allowing much smaller IP sizes, together with very little emittance growth, relaxing the requirements on beam current and damping time.

These studies are still in progress.

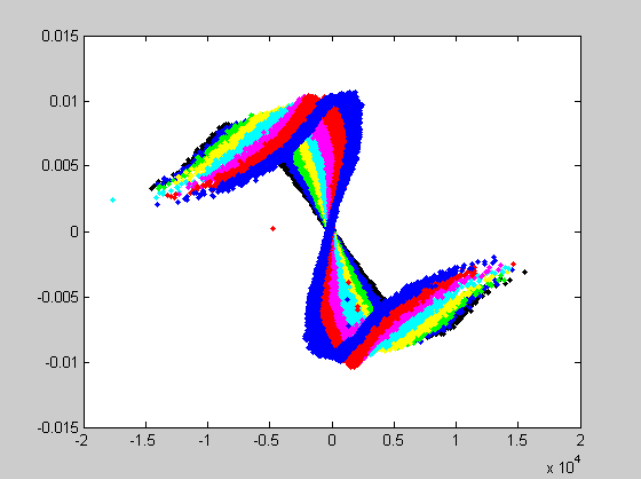


FIG. 18: Plot of the HER $(x, x')$ phase space. Each color refers to one longitudinal bunch slice.

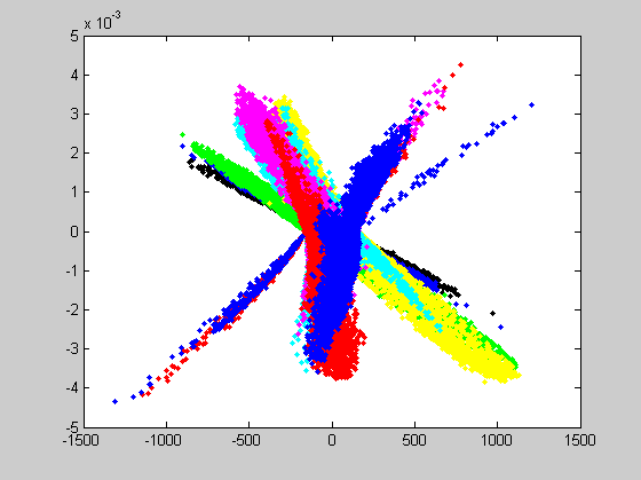


FIG. 19: Plot of the HER $(y, y')$ phase space. Each color refers to one longitudinal bunch slice.

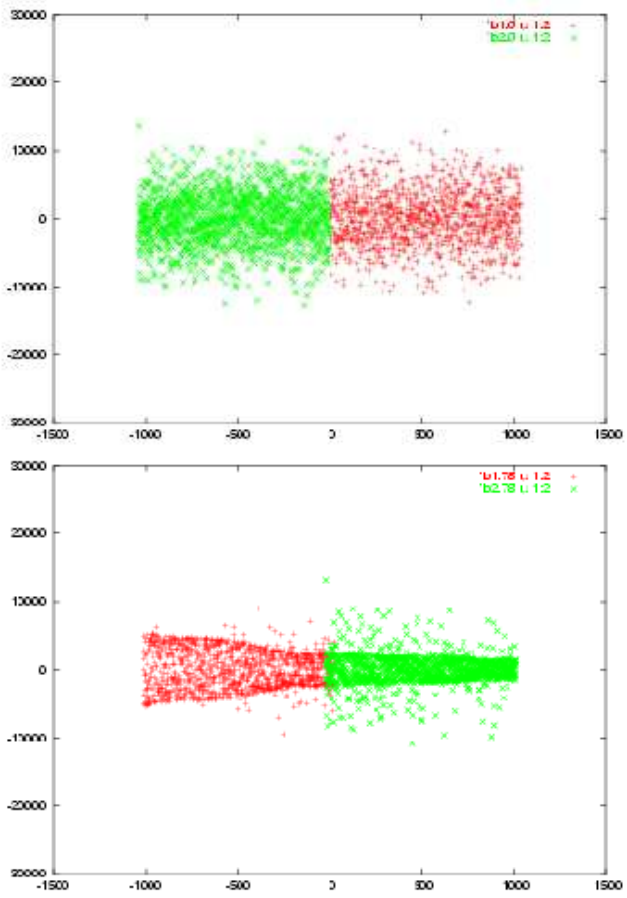


FIG. 20: Beams before (top) and after (bottom) collision: horizontal vs longitudinal (z) distribution. LER particles are red, HER particles are green.

## 20. INTERACTION REGION PARAMETERS

The interaction region is being designed to leave the same longitudinal free space as that presently used by *BABAR* but with superconducting quadrupole doublets as close to the interaction region as possible.

Recent work at Brookhaven National Laboratory on precision conductor placement of superconductors in large-bore low-field magnets has led to quadrupoles in successful use in the interaction regions for the HERA collider in Germany [26]. A minor redesign of these magnets will work well for the Super *B* Factory.

The reduced energy asymmetry (7 GeV×4 GeV) of the SuperB factory makes it extremely difficult to separate the beams, especially if the collision is head-on. However, the low emittance of the incoming beams helps since the magnetic apertures can be small. On the other hand, the exiting disrupted beams need large aperture magnets to contain the beam with a minimum of loss. The reduced collision frequency (100 kHz – 1 MHz) of the SuperB Factory permits the introduction of pulsed magnetic elements.

The plan to collide the two beams head-on and let the exiting beam travel through the two final focus magnets of the other beam. The exiting high-energy beam will be underfocused by the incoming low-energy beam (LEB) final focus magnets. Two pulsed quadrupole magnets will be used to add additional focusing for the outgoing high-energy beam (HEB). These pulsed magnets will operate only on the outgoing HEB and not be energized for the incoming LEB. The incoming LEB will be steered to the final focus trajectory by a pulsed dipole that will be outboard of the pulsed quadrupoles mentioned above. The pulsed dipole on the incoming LEB allows the beams to be separated and the out-going HEB then enters its own beam pipe.

On the other side of the IP the outgoing LEB is overfocused by the incoming HEB final focus magnets. Again two pulsed quadrupole magnets will be used to help capture the disrupted LEB. The LEB is then steered out of the way by a pulsed dipole magnet allowing it to enter its own beam

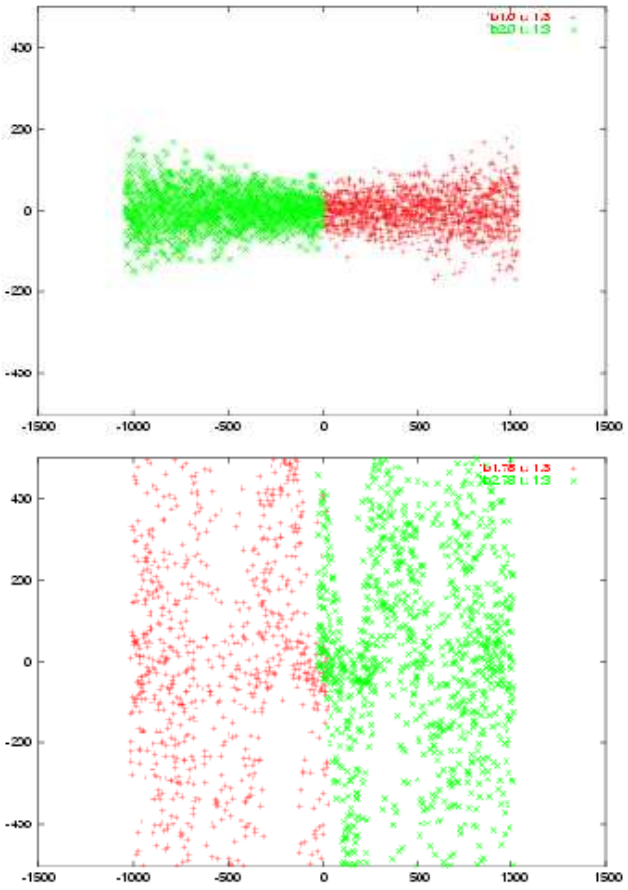

FIG. 21: Beams before (top) and after (bottom) collision: vertical vs longitudinal (z) distribution. LER particles are red, HER particles are green.

pipe.

This design minimizes synchrotron radiation (SR) generated by the HEB since the HEB runs straight through the Interaction Region (IR). The SR fan from the incoming LEB pulsed dipole must be shielded from the detector beam pipe. The remaining primary sources of SR that can be a background for the detector, are generated by the final focus quadrupoles for both incoming beams. This SR must be masked from the detector beam pipe as well. The low emittance of the incoming beams allows us to have a radius for the detector beam pipe of about 1 cm.

The masking for the detector beam pipe will be close to the beam pipe in Z. This means that there will be scattered photons from the mask tips and (most likely) photons striking the inside surfaces of the masks from SR generated from the incoming beam on the other side of the IP. This means that the detector Be beam pipe will need to have the inside surface coated with a high-Z material (most likely gold) in order to minimize the SR background in the detector.

Fig. 7 shows a possible IR layout. After passing through the collision point (IP) HER and the LER beams are then steered away from the incoming beam magnets with fast kicker dipole magnet. The RF quads would turn on right after the incoming beam passes by.

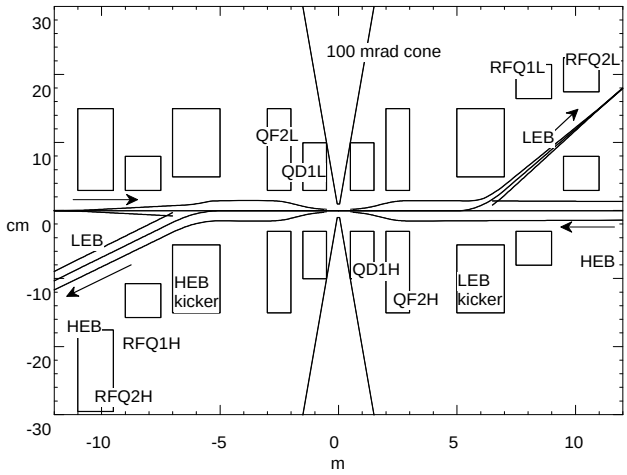


FIG. 22: Plan view of a possible IR design.

## 21. LINAC PARAMETERS

The SC linear accelerator will have a design similar to the International Linear Collider (ILC) SC structures with a frequency of 1428 MHz. Higher Order mode (HOM) damping will be needed similar to the ILC. Since these structures will be powered at all times, an accelerating gradient of about 8 MV/m is assumed here with a filling factor of 0.7 similar to the ILC. Thus, a tunnel length of about 200 m is needed for each GeV of acceleration including beam loading. The klystron power needed here will be much lower than the ILC as the energy is recovered for each bunch.

## 22. DAMPING RING PARAMETERS

The damping rings for each beam will have a total circumference if 6 km but two 3 km rings per particle type may be better. The first ring will have a very short damping time to reduce the transverse emittance. It will have a relatively large energy loss and large equilibrium emittances. The second ring will have softer bends to have smaller final emittances. Preliminary damping ring parameters are listed in Table VII.

Their characteristics are very similar to the ones studied for ILC [23]. The ILC-DR has the same length and emittances very similar to the ones required for the Super-B. The ILC damping time is longer, so more wigglers are needed here. A careful re-optimization of the ring lattice has to be done in order to have a good dynamic aperture. The additional wigglers together with the increased beam current circulating in the ring (about a factor 5) will be a serious concern for the electron-cloud instability. The other collective effects will also be worse, despise the small benefit from the shorter damping time. In addition we would like to have the

rings operate at low energy, to same power and cost, the design energy will be chosen after a careful study, and probably will not be much lower than 2 GeV.

TABLE VII: Preliminary Damping Ring Parameters.

| **Parameter** | **LEB** |
|---|---|
| Energy (GeV) | 2 |
| Circumference (m) | 3000 |
| Number of rings | 2 |
| Average sync loss per turn MeV | 4.7 |
| Total Synchrotron Rad Power MW/ring | 19 |
| RF frequency (MHz) | 476 |
| Vertical tune | 72.21 |
| Horizontal tune | 76.29 |
| Current (A) | 8 |
| Bunches/ring | 5000 |
| Particles per bunch | $1\times10^{11}$ |
| Ion gap (%) | 1 |
| Energy spread (%) | 0.02 |
| HER RF volts (MV) | 25 |
| Longitudinal Damping time (msec) | 4.3 |
| Emittance (x/y) (nm) | 0.7/0.0016 |
| $\sigma_z$ (mm) | 3 |

## 23. INJECTOR CONCEPT AND PARAMETERS

The injector for the SuperB will make up for lost particles during the storage time in the damping rings and the losses from collisions. The injector will be similar to the SLAC injector delivering about $5\times10^{10}$ electrons or positrons per pulse at about 40 Hz each.

## 24. BUNCH COMPRESSION

The bunch compression system needs to compress the bunches between a factor of 5 to 10 from 2-3 mm to 0.4-0.3 mm. Compression is done by adding an head-tail energy correlation in each bunch and then passing it through a transport line with dispersion. Since the initial energy spread in the damping rings is very small, the induced energy spread for compression will be about $1\times10^{-3}$. Perhaps a multi-stage compressor like in ILC will be required. The compressor could be integrated with the SC accelerator in order to fully optimize the bunch length, its profile (a rectangular distribution is probably desired) and the final energy spread. The average dispersion needs to be about 1 m over a bend angle of about 3 radians.

## 25. POWER REQUIREMENTS

The power required by a collider is the sum of a site base and the accelerator operation. The damping ring power to replace the synchrotron radiation loss will be the dominate factor in this Super-B Factory. The SC linac with energy recovery of the beams will not be a large source.

## 26. SYNERGY WITH ILC

There are many similarities between this linear Super-B collider and the ILC. The project described here will capitalize on R&D projects that have been concluded or are ongoing with the ILC collaboration.

The damping rings between the two projects are very similar. Many of the parameters are close such as energy (2-5 GeV), circumference (3-6 km), bunch spacing (3-8 nsec), damping times (4-10 msec), and emittances (3-10 nm horizontally and 0.002-0.001 nm vertically). Most of the beam dynamics are due to multi-bunch effects which affect both designs. The electron cloud effects will affect both rings in a similar fashion. Both RF frequencies are in the range of 400 to 700 MHz.

The SC linacs have very similar characteristics including gradients (5-25 MV/m), bunch spacing ($\sim$ 300 nsec), and bunch charges ($1\text{-}10\times10^{10}$).

The interaction regions have very similar characteristics with flat beams and geometries. The ratio of IP beta functions are nearly the same (10-30 mm horizontally and 0.3-1 mm vertically). The collimation schemes should be similar. The possibility and techniques to use traveling focusing will be similar, if needed. The chromatic corrections of the final doublets using sextupoles will be the same.

All the beams will need bunch-by-bunch feedbacks to keep the beam instabilities and beam-beam collisions under control. With the bunch spacing very similar, the feedback kickers, digital controls, and beam impedance remediation will have common designs. The IP feedback from bunch-to-bunch will work exactly in the same way except that the required SuperB Factory magnets will be much weaker. There will be many opportunities to use feed-forward to correct bunch steering in advance of the bunch arrival in the SuperB design.

## 27. OTHER UPGRADE POSSIBILITIES

Additional improvements are being considered for this design.

1) A traveling focus scheme in the interaction region could help the beam-bean interaction and increase the luminosity or reduce the beam-beam blowup allowing the bunches to collide more frequently.

2) A monochromator scheme could be used to reduce the energy spread tolerances in the interaction region and allow a simpler damping ring or enhanced luminosity.

3) The SC linac could be "doubled up" to be used by more than one beam to reduce the construction cost.

4) A four-beam collision scheme could be used to significantly reduce the effects of the beam-beam interaction allowing a much higher collision rate.

## 28. ACKNOWLEDGMENTS

This document has come out of several recent SuperB workshops, with the most recent one being at LNF (Frascati) on Nov. 11-12, 2005. We appreciate very much discussions with the participants in these workshops. We also appreciate discussions of parameters with members of the ILC collaboration.

[1] B. Aubert *et al.* [*BABAR* Collaboration], Phys. Rev. Lett. **94** (2005) 161803; K. Abe *et al.* [*Belle* Collaboration], Phys. Rev. D **71** (2005) 072003 [Erratum-ibid. D **71** (2005) 079903].

[2] B. Aubert *et al.* [*BABAR* Collaboration], arXiv:hep-ex/0507017. B. Aubert *et al.* [*BABAR* Collaboration], Phys. Rev. Lett. **95** (2005) 111801 [arXiv:hep-ex/0506036]. I. Bizjak *et al.* [*Belle* Collaboration], arXiv:hep-ex/0505088. A. Limosani *et al.* [*Belle* Collaboration], Phys. Lett. B **621** (2005) 28 [arXiv:hep-ex/0504046]. B. Aubert *et al.* [*BABAR* Collaboration], arXiv:hep-ex/0506065. B. Aubert *et al.* [*BABAR* Collaboration], arXiv:hep-ex/0507085. B. Aubert *et al.* [*BABAR* Collaboration], arXiv:hep-ex/0506064. B. Aubert *et al.* [*BABAR* Collaboration], arXiv:hep-ex/0507085. B. Aubert *et al.* [*BABAR* Collaboration], arXiv:hep-ex/0507003.

[3] K. Abe [*Belle* Collaboration], arXiv:hep-ex/0507037.

[4] B. Aubert *et al.* [*BABAR* Collaboration], Phys. Rev. Lett. **95** (2005) 041805 [arXiv:hep-ex/0503049]. K. Abe *et al.*, arXiv:hep-ex/0507039.

[5] K. Abe *et al.*, arXiv:hep-ex/0508048. B. Aubert *et al.* [*BABAR* Collaboration], arXiv:hep-ex/0508001. K. Abe *et al.* [*Belle* Collaboration], arXiv:hep-ex/0504013. B. Aubert *et al.* [*BABAR* Collaboration], arXiv:hep-ex/0507101.

[6] J. Charles *et al.* [CKMfitter Group], Eur. Phys. J. C **41** (2005) 1; M. Bona *et al.* [UTfit Collaboration], JHEP **07** (2005) 028. See also `http://ckmfitter.in2p3.fr/` and `http://www.utfit.org` for updates to current data.

[7] J. M. Soares and L. Wolfenstein, Phys. Rev. D **47** (1993) 1021. N. G. Deshpande, B. Dutta and S. Oh, Phys. Rev. Lett. **77** (1996) 4499 [arXiv:hep-ph/9608231]. J. P. Silva and L. Wolfenstein, Phys. Rev. D **55** (1997) 5331 [arXiv:hep-ph/9610208]. A. G. Cohen, D. B. Kaplan, F. Lepeintre and A. E. Nelson, Phys. Rev. Lett. **78** (1997) 2300 [arXiv:hep-ph/9610252]. Y. Grossman, Y. Nir and M. P. Worah, Phys. Lett. B **407** (1997) 307 [arXiv:hep-ph/9704287]. M. Ciuchini, E. Franco, F. Parodi, V. Lubicz, L. Silvestrini and A. Stocchi, eConf **C0304052** (2003) WG306 [arXiv:hep-ph/0307195]. S. Laplace, Z. Ligeti, Y. Nir and G. Perez, Phys. Rev. D **65** (2002) 094040 [arXiv:hep-ph/0202010].

[8] M. Bona *et al.* [UTfit Collaboration], arXiv:hep-ph/0509219.

[9] B. Aubert *et al.* [BaBar Collaboration], Phys. Rev. Lett. **93** (2004) 131801 [arXiv:hep-ex/0407057]. K. Abe *et al.*, arXiv:hep-ex/0507045. A. Warburton [CDF Collaboration], Int. J. Mod. Phys. A **20** (2005) 3554 [arXiv:hep-ex/0411079].

[10] Y. Grossman and M. P. Worah, Phys. Lett. B **395** (1997) 241 [arXiv:hep-ph/9612269]; M. Ciuchini, E. Franco, G. Martinelli, A. Masiero and L. Silvestrini, Phys. Rev. Lett. **79** (1997) 978 [arXiv:hep-ph/9704274]; D. London and A. Soni, Phys. Lett. B **407** (1997) 61 [arXiv:hep-ph/9704277]. Y. Grossman, G. Isidori and M. P. Worah, Phys. Rev. D **58** (1998) 057504 [arXiv:hep-ph/9708305].

[11] B. Aubert *et al.* [*BABAR* Collaboration], Phys. Rev. D **71** (2005) 091102 [arXiv:hep-ex/0502019]. K. Abe *et al.* [*Belle* Collaboration], arXiv:hep-ex/0507037. B. Aubert *et al.* [*BABAR* Collaboration], arXiv:hep-ex/0507087. B. Aubert *et al.* [*BABAR* Collaboration], arXiv:hep-ex/0408095. B. Aubert *et al.* [*BABAR* Collaboration], Phys. Rev. D **71** (2005) 111102 [arXiv:hep-ex/0503011]. B. Aubert *et al.* [*BABAR* Collaboration], arXiv:hep-ex/0508017. B. Aubert *et al.* [*BABAR* Collaboration], arXiv:hep-ex/0503018. B. Aubert *et al.* [*BABAR* Collaboration], arXiv:hep-ex/0507016. B. Aubert *et al.* [*BABAR* Collaboration], arXiv:hep-ex/0507052.

[12] M. Beneke, Phys. Lett. B **620** (2005) 143 [arXiv:hep-ph/0505075]. H. Y. Cheng, C. K. Chua and A. Soni, Phys. Rev. D **72** (2005) 094003 [arXiv:hep-ph/0506268]. G. Engelhard and G. Raz, arXiv:hep-ph/0508046. Y. Grossman, Z. Ligeti, Y. Nir and H. Quinn, Phys. Rev. D **68** (2003) 015004 [arXiv:hep-ph/0303171]. M. Gronau, Y. Grossman and J. L. Rosner, Phys. Lett. B **579** (2004) 331 [arXiv:hep-ph/0310020]. M. Gronau, J. L. Rosner and J. Zupan, Phys. Lett. B **596** (2004) 107 [arXiv:hep-ph/0403287]. G. Engelhard, Y. Nir and G. Raz, Phys. Rev. D **72** (2005) 075013 [arXiv:hep-ph/0505194].

[13] G. Buchalla, G. Hiller, Y. Nir and G. Raz, JHEP **0509** (2005) 074 [arXiv:hep-ph/0503151].

[14] M. Ciuchini, E. Franco, G. Martinelli, A. Masiero and L. Silvestrini, Phys. Rev. Lett. **79** (1997) 978 [arXiv:hep-ph/9704274]. M. Ciuchini, E. Franco, A. Masiero and L. Silvestrini, arXiv:hep-ph/0307194. For a recent update, see L. Silvestrini, arXiv:hep-ph/0510077.

[15] L. J. Hall, V. A. Kostelecky and S. Raby, Nucl. Phys. B **267** (1986) 415.

[16] A. J. Buras, P. Gambino, M. Gorbahn, S. Jager and L. Silvestrini, Phys. Lett. B **500** (2001) 161 [arXiv:hep-ph/0007085].

[17] G. D'Ambrosio, G. F. Giudice, G. Isidori and A. Strumia, Nucl. Phys. B **645** (2002) 155 [arXiv:hep-ph/0207036].

[18] For a recent analysis, see C. Bobeth, M. Bona, A. J. Buras, T. Ewerth, M. Pierini, L. Silvestrini and A. Weiler, arXiv:hep-ph/0505110, accepted by Nucl. Phys. B.

[19] M. Ciuchini, A. Masiero, L. Silvestrini, S. K. Vempati and O. Vives, Phys. Rev. Lett. **92** (2004) 071801 [arXiv:hep-ph/0307191].

[20] KEKB Status report PAC 2005 Knoxville, TN.

[21] PEP-II Status report PAC2005 Knoxville, TN.

[22] The SLC Design Handbook, SLAC November 1984.

[23] International Linear Collider Technical Review Committee, Second Report 2003, ICFA SLAC-R-606.

[24] D. Schulte, "Study of electromagnetic and hadronic background in the Interaction Region of the TESLA Collider", PhD Thesis, Hamburg, 1996.

[25] J. Le Duff et al., "Space charge compensation with DCI", XI Int. Conf. on High Energy Accelerators, CERN, July 1980.

[26] B. Parker et al., "Superconducting Magnets for use inside the HERA ep Interaction Regions," PAC 1999, New York, p. 308.